

1. Introduction

1.1 Quantitative Structure Activity Relationship (QSAR)

Quantitative structure activity relationships (QSARs), are the part of science which study the interface between chemistry and biology, it is one of the new fields of biomedical research which increase rapidly since its beginnings in the 1960. QSARs was initiated by the pioneering work of Corwin Hansch and other researchers, who found the way to combine two areas that seemed to be far apart; physical chemistry and biology. The tool that used in such operation was mathematical modelling which is meant mathematical descriptions using a relatively small number of well tested parameters and graphics to make the connections. QSARs analysis, permitting the quantitative study of the interaction between chemicals and life, has been applied with success in many different areas. The use of QSARs has become very popular in the field of rational design of drugs and pesticides because it supports faster and more efficient design. It also provides information on web based resources of carcinogenicity and mutagenicity data and issues pertaining to the use of these data in QSAR study. To offer a wider perspective, a comparison is made between QSAR models for mutagenicity and carcinogenicity and those for the environmental toxicity of the chemicals. The potential and limitations of QSAR models as supporting tools for risk assessment are treated extensively. (Benigni, 2003) . In QSAR analysis, one or more molecular descriptors are related with the molecular activity by using a statistical analysis. The main objective of this analysis is the producing statistical models through which it is possible to predict the biological activity of novel compounds that have not been tested yet or even cannot be determined. The main steps involved in the development of a QSAR model are the selection of the database of compounds with known biological activities (training set), the calculation of molecular descriptors, the development of a statistical model that relates the activity with the calculated descriptors, then the evaluation of the generated model with a test set. The molecular descriptors consist in a series of numerical values associated, for example, with the structural, electronic, steric, or physicochemical properties of the molecular system in study. At the present, a great number of molecular descriptors have been conceived among which, topological indices, as well as quantum chemicals topographic and physicochemical descriptors. For the calculation of the topographic and quantum chemical descriptors it is necessary to determine the most stable 3D structure of the compounds through molecular mechanics or semi empirical calculations in combination with methods of conformational. QSAR models with molecular connectivity indices and (MCIs) were particularly successful in estimating various partitioning properties of persistent organic pollutants (POPs) which are described by UN Environment Programme (UNEP) as one of the great environmental challenges the world faces. Typical examples of those chemicals are polychlorinated biphenyls (PCBs), polychlorinated dibenzodioxins and dibenzofuranes (Sabljic, 2001 ; Vilar *et al*, 2008)

1.2. Multiple linear regressions

MLR generates QSAR equations by performing standard multivariable regression calculations to identify the dependence of a drug property on any or all of the descriptors under investigation. The possibility of chance correlation is checked through the values of multiple correlation coefficient (r), Student's t-value; Fisher's F ratio, standard deviation (s), and through independent tests like the leave-one-out (LOO) method. The significance of correlation can be judged through cross-validated correlation coefficient (r^2_{cv} or q^2) values and also by the y-scrambling technique. MLR assumes that all variable is independent, and not correlated. However, in the multivariate case, i.e., MLR analysis involving more than one independent variable, the relationship is expressed with the following single multiple term linear equations:

$$y = b_0 + b^1 x^1 + b^2 x^2 + \dots + b_m x_m + e$$

the MLR analysis estimates the regression coefficients (b_i), by minimizing the residual error (e), which quantify the deviation of a particular point from the regression line, as in the case of simple linear regression. (Verma *et al*, 2010)

1.3. Molecular Operating Environment (MOE):

Macromolecular crystallographic data, when available, can be a valuable source of information for discovering active ligands. MOE provides a collection of applications for visualizing and understanding details of receptor active sites and receptor-ligand interactions. These applications are used to suggest improvements to ligands or screen ligand databases for candidate binders. Detect and score candidate protein-ligand and protein-protein binding sites using a fast α -shapes algorithm. The sites are scored for Ligand Binding Propensity (Soga, 2007). Visualize individual sites or populate them with "dummy atoms" for docking calculations or starting points for de novo ligand design efforts. Visualize the residues in close contact with a ligand or series of ligands in diagram format [Clark, 2007]. Identify hydrogen bonds, salt bridges, hydrophobic interactions, cation π , sulphur LP, halogen bonds and solvent exposure. Browse through a chemical series or receptor family series to identify conserved or non-conserved interactions for selectivity analysis. Dock small molecules in a macromolecular binding site. Supply a database of conformations or generate conformations on the fly. Choose between various scoring functions and optionally constrain the generated poses to satisfy a pharmacophore query to bias the search towards known important interactions. Use the streamlined scenario-based interface for docking covalent ligands, running electron density guided docking or knowledge-based template guided docking scoring or a fast grid based method (Labute, 2008). An interface to third party docking programs is provided for high throughput virtual screening. The docking architecture is parallelized using the MOE technology (Corbeil, 2012).

Multi-Fragment Search is an ensemble-based method for mapping the preferred locations of specific chemical groups in a receptor structure (Miranker, 1991). An

active site of a macromolecular structure is populated with a large number of chemical fragments, which are subjected to an energy minimization protocol. The resulting group locations are clustered, scored (including solvation effects) and written to a database for subsequent visualization and analysis.

Automated Structure Preparation Automatically correct many problems encountered in crystallographic data such as missing loops, empty residues, chain termini or breaks, missing disulfide bonds or atom names, picking alternate conformations, etc using the Structure Preparation application. Optimize the hydrogen bonding network by navigating through different tautomer/protomer states or automatically by using Protonate3D. Protonate3D calculates optimal protonation states, including titration, rotamer and “flips” using a large-scale combinatorial search (Labute, 2008).

1.4. Docking

Molecular Docking is the process that involves placing molecules in appropriate configurations to interact with a receptor. Molecular Docking is a natural process which occurs within seconds in a cell. In the field of molecular modelling, molecular Docking is a method which predicts the preferred orientation of one molecule to second when bound to each other to form a stable complex. Knowledge of the preferred orientation is used to predict the strength of association or binding affinity between two molecules using scoring functions. The associations between biologically relevant molecules such as proteins, nucleic acids, carbohydrates, and lipids play central role in signal transduction. Furthermore, the relative orientation of the two interacting partners may affect the type of signal produced. Therefore docking is useful for predicting both the strength and type of signal produced. Docking is frequently used to predict the binding orientation of drug candidates to their protein targets in order to predict the affinity and activity of the small molecule. Hence Docking plays an important role in the rational design of drugs. Molecular recognition plays a key role in promoting fundamental biomolecular events such as enzyme substrate, drug-protein and drug-nucleic acid interactions. Detailed understanding of the general principles that govern the nature of the interactions (Van der Waals, hydrogen bonding, electrostatic) between the ligands and their protein or nucleic acid targets may provide a framework for designing the desired potency and specificity of potential drug leads for a given therapeutic target. Practical application of this knowledge requires structural data for the target of interest and a procedure for evaluating candidate ligands. (Phillips *et al*, 2005).

1.5. Computational chemistry

Computational chemistry is usually used when a mathematical method is sufficiently well developed that it can be automated for implementation on a computer. Computational chemistry is the application of chemical, mathematical and computing skills to the solution of interesting chemical problems. It uses computers to generate information such as properties of molecules or simulated experimental results. Very few aspects of chemistry can be computed exactly, but almost every aspect of chemistry has been described in a qualitative or approximate quantitative computational scheme. However, just as not all spectra are perfectly resolved, often a qualitative or approximate computation can give useful insight into chemistry. Computational chemistry has become a useful way to investigate materials that are too difficult to find or too expensive to purchase. It also helps chemists make predictions before running the actual experiments so that they can be better prepared for making observations (Young, 2001). Computational chemistry is a set of techniques for investigating chemical problems on a computer.

Questions commonly investigated computationally are:

Molecular geometry: The shapes of molecules, bond lengths, angles, and dihedrals.

Energies of molecules and transition states: This tells us which isomer is favoured at equilibrium, and (from transition state and reactant energies) how fast a reaction should go.

Chemical reactivity: For example, knowing where the electrons are concentrated (nucleophilic sites) and where they want to go (electrophilic sites) enables us to predict where various kinds of reagents will attack a molecule.

IR, UV, and NMR spectra: These can be calculated, and if the molecule is unknown, someone trying to make it known what to look for.

The interaction of a substrate with an enzyme: Seeing how a molecule fits into the active site of an enzyme is one approach to designing better drugs.

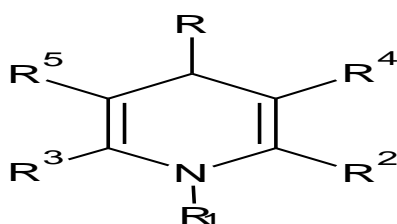
The physical properties of substances: These depend on the properties of individual molecules and on how the molecules interact in the bulk material. For example, the strength and melting point of a polymer (e.g. a plastic) depend on how well the molecules fit together and on how strong the forces between them are. (Lewars and Errol, 2004).

1.5.1 Computational Tools

The search for new compounds with a given biological activity requires enormous effort in terms of manpower and cost. This effort arises from the large number of compounds that need to be synthesized and subsequently biologically evaluated. For this reason, the pharmaceutical industry has shown great interest in theoretical

methods that enable the rational design of pharmaceutical agents. In the last years bioinformatics has experienced a great evolution due to the development of specialized software and to the increasing computer power. The codification of the structural information of molecules through molecular descriptors and the subsequent data analysis allow establishing QSAR models (Quantitative Structure-Activity Relationship) that can be applied to the design and the virtual screening of new drugs. The development of sophisticated Docking methodologies also allows a more accurate predict of the biological activity of molecules. Moreover, through this type of computational techniques and theoretical approaches, it is possible to develop explanatory hypothesis on the mechanism of action of drugs (Vilar et al, 2008).

1.6. 1,4-dihydropyridine

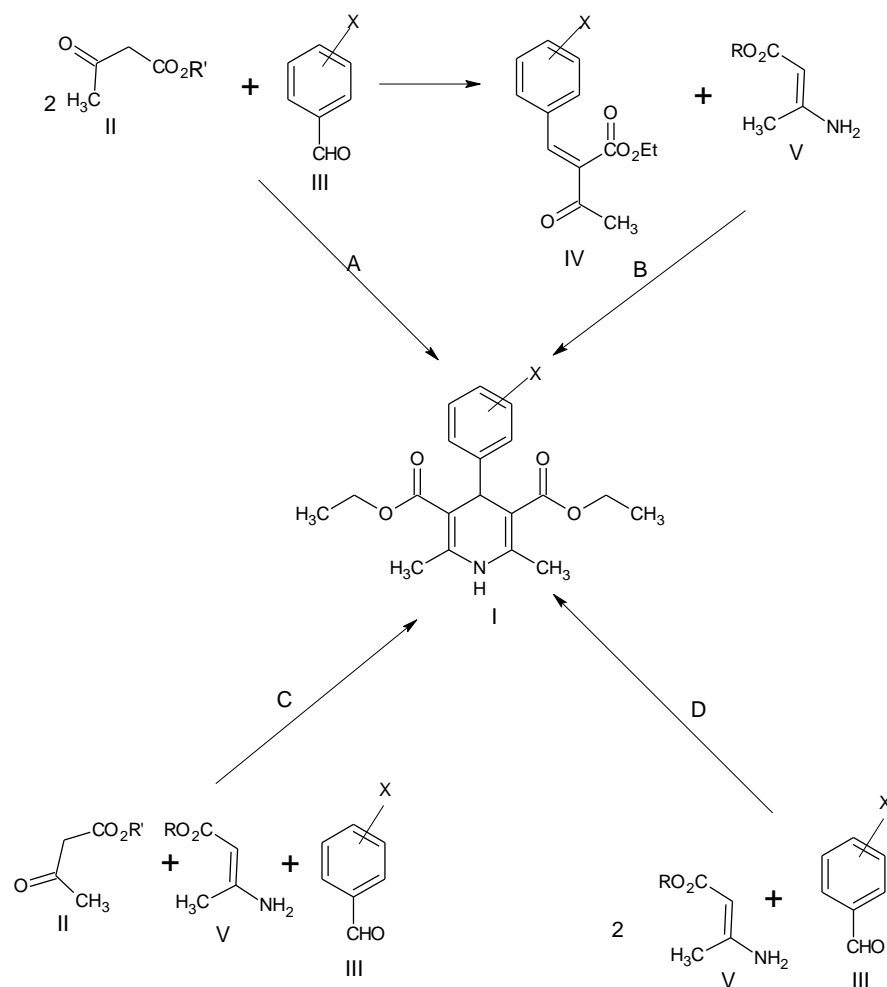


1,4-dihydropyridine is an intrinsic structural part of many pharmacologically active compounds and drugs. Introduction and variation of the substituents at the 1,4-dihydropyridine ring can result in elaboration of the compounds which can be capable to interact at diverse receptors and ion channels. In the same way these activities depend on various structural parameters related to dihydropyridine (presence and character of substituents), lipophilicity, and depth of the incorporation in the biological membranes. Additionally, the main structure element dihydropyridine cycle can be regarded as a model of the redox coenzyme NADPH or as analogue of 1,4-dihydronicotinic amide. 1,4-dihydropyridines regulate redox reactions, possess free radical scavenging properties, inhibit the peroxidation processes and protect biological membranes. Since the end of the last century in the fields of medicinal and pharmaceutical sciences efforts directed toward the development of new technologies, including transport systems have increased significantly. Synthetic delivery systems most frequently are formed on amphiphilic compound basis such as cationic lipids, etc. However, there is no sufficient data concerning to characterization of formed nanoparticles and the relationships between delivery-activity and properties of Nano systems. Heterocyclic are central backbones of the main of natural products, pharmaceutically active molecules and biologically relevant compounds, 1,4-dihydropyridine is privileged nitrogen containing heterocyclic which showed up everywhere in drugs currently in use clinics and biologically active compounds. 1,4-dihydropyridines exhibit various activities such as the calcium channel antagonists. Dihydropyridines act by inhibiting the influx of calcium ion into the vascular smooth muscle cells via L-type calcium channels their useful effects in management of cardiovascular disorders are due to their ability to relax vascular smooth muscles. In

angina pectoris, such drugs decrease the resistance in systemic and coronary arterial beds, thereby reducing cardiac oxygen requirement and increasing cardiac oxygen supply, respectively (Kumar *et al*, 2011; Datar and Auti, 2016). Therefore, the preparation of novel 1,4-DHP derivatives is challenging target in medicinal and synthetic organic chemistry. Many attempts to improve Hantzsch synthesis using green methods and alternative catalysts have been studied, the most efficient strategies for the synthesis of 1,4-DHPs are multicomponent reactions (MCRs) in terms of providing both sufficient structural diversity and many compounds libraries. (Rucins Martins, 2017). Hantzsch 1,4-dihydropyridines (dialkyl 1,4-dihydro-2,6-dimethylpyridine-3,5-dicarboxylates) are widely used clinically as calcium channel blockers for the treatment of cardiovascular diseases, such as, nifedipine and nitrendipine are used for the treatment of hypertension and angina pectoris, nifedipine is a potent vasodilator and nimodipine exhibits selectivity for cerebral vasculature. DHP derivatives are employed as potential drug candidates for the treatment of congestive heart failure. The success of those calcium antagonists has led to the development of novel synthetic strategies to improve their classical methods of preparation. (Kumar *et al*, 2011).

1.6.1. Synthesis of 1,4-Dihydropyridine

1,4-DHPs as the cyclic base donors are known as useful reactants in the synthesis of complex organic molecules. A common feature of most known multicomponent methods, however, is that an aldehyde must be used to donate the formyl group. Such kind of synthetic methods result in the consequence of limited product diversity since most known multicomponent 1,4-DHPs syntheses provide 4-aryl or 4-alkyl 1,4-DHPs by relying on the aldehyde as the donor of C-4 fragment of the ring.



Scheme 1 Most common variation of Hantzsch 1,4-dihydropyridine synthesis

As it seen from the figure 1, methods **A** (aldehyde **III** and two equivalents of Ethyl acetoacetate **II**), while methods **B** (two step synthesis *via* Knoevenagel intermediate **IV** and β -aminocrotonic acid ester **V**), in the methods **C** (three component cyclocondensation; aldehyde **III**, acetoacetic acid ester **II** and β -aminocrotonic acid ester **V**) are usually used for the synthesis of 1,4-DHPs having different ester moieties ($R \neq R'$) and the methods **D** (aldehyde **III** and two equivalents of β -amino crotonic acid ester **V**) are only used for the synthesis of 1,4-DHPs ($R=R'$) (Rucins Martins, 2017),

1.7. Biological Activity of 1,4 Dihydropyridine

Dihydropyridine is a molecule based upon pyridine, and the parent of a class of molecules that have been semi-saturated with two substituents replacing one double bond. They are particularly well known in pharmacology as L-type calcium channel blockers, used in the treatment of hypertension. Compared with certain other L-type calcium channel blockers (for example those of the phenylalkylamine class such as verapamil) that have significant action at the heart, they are relatively vascular selective in their mechanism of action in lowering blood pressure.

A new series of 1,4-dihydropyridine derivatives was synthesized, The synthesized compounds showed activity more than ciprofloxacin against *S. aureus* organism and more active than clotrimazole against *C. albicans*. compound synthesized by Kumar and his team in 2010, they were used condensation to prepare a series of 1,4-dihydropyridine derivatives, their compound found to be active against three type of anticancer (Kumar *et al*).

A new series of 1,4-dihydropyridine derivatives were synthesized via ultrasound irradiation and evaluated for antimicrobial and anticoagulant activities by (Ahamed et al. 2017).

A novel 4-substituted 1,4-dihydropyridine derivatives were designed and synthesized by (Datar and Auti,2012). Like other analogues of nifedipine, they were lipophilic compounds and reduced the mean arterial blood pressure.

(Mehta and Verma,2012) synthesised anew series of 1,4-dihydropyridine derivatives and screened in vitro antibacterial activity against Gram(-) and Gram(+) organisms.

A series of N-(6-nitrobenzothiazolyl)-2,3,5,6-tetrasubstituted-4-(aryl)-1,4-dihydropyridines were synthesized by (Mithlesh et. al,2011). All compounds were tested for antibacterial and antifungal activities and results have been compared with standard drugs.

1.8. Research Objective

1.8.1. Main Objective

The main objective of the conducted study is to use quantitative structure–activity relationships (QSARs) to synthesis a derivative of 1,4 dihydropyridine that have efficacy against liver cancer.

1.8.2. Specific Objectives

1/using molecular modelling to designing some derivatives of 1,4 dihydropyridine and find out their descriptors

2/ To study quantitative structure–activity relationships (QSARs) for 1,4 dihydropyridine as anti-cancer agents

3/To perform molecular docking which shows the interaction between designed molecule with high R^2 value from QSAR equation

4/To synthesize a derivatives of 1,4 dihydropyridine which have efficacy against liver cancer from docking and QSAR studies .

5/ To predict biological activity of synthesized compounds by using the equation of QSAR.

6/ To compare predicted biological activity with real biological activity.

2. Materials and Methods

2.1. Chemicals

Ethyl aceto acetate $\text{CH}_3\text{COCH}_2\text{COOCH}_2\text{CH}_3$, Density 1.028-1.030g/cm³, Assay 98%, Alpha CHEMIKA, India

Acetaldehyde, Density 0.778g/cm³, Assay 20-30%, CDH Laboratory reagent, India.

Benzaldehyde $\text{C}_6\text{H}_5\text{CHO}$, Density 1.044-1.047g/cm³, Assay 98.5-99.5%, LOBA Chemie, India.

Salicylaldehyde $\text{C}_7\text{H}_6\text{O}_2$, Density 1.164-1.167g/cm³, Assay 99%, LOBA Chemie, India.

Vanillin $\text{C}_8\text{H}_8\text{O}_3$, Assay 99%

Ethanol ($\text{C}_2\text{H}_5\text{OH}$), Density 0.808-0.812 g/cm³, Assay 94.8-95.8%, duksan pure chemical, KOREA.

Diethyl ether $\text{C}_4\text{H}_{10}\text{O}$, Density 0.713-0.717 g/cm³, Assay 98%, LOBA Chemie, India.

P-bromo Aniline $\text{C}_6\text{H}_6\text{NBr}$, Assay 98%, LOBA Chemie, India.

Ammonium Acetate, Assay 98%, LOBA Chemie, India.

Chemicals were used without further purification.

2.2. Apparatus and Equipment:

Analog water bath, Scott Science, UK.

Melting Point apparatus, Gallenkamp, England.

Sensitive balance, Adam equipment, South Africa

2.3. Glassware:

All glassware's were Pyrex type.

2.4. Thin-Layer Chromatography (TLC)

Thin-layer chromatography (TLC) was carried out using pre-coated LK5DF silica gel 150A plate (size 5×20 cm, 250 μm layer) obtained from Whatman Inc, New Jersey, USA using 98% chloroform and 2% methanol as an eluent and the spots were visualized by iodine vapours/ultraviolet light as visualizing agents.

2.5. Instrumentations:

2.5.1. Infra-Red Spectrophotometer (IR)

IR spectral analysis was carried out using FTIR-8400s spectrophotometer obtained from (SHIMADZU, Japan) in KBr pellets.

2.5.2. Ultraviolet-Visible Spectrophotometer (UV-VIS)

Ultraviolet spectral data analysis was carried out using 6505 UV-VIS spectrophotometer Jenway, England.

2.6. Software's:

2.6.1 ACD lab program

acd/lab free ware 2012 from www.acdlabs.com.

2.6.2 Minitab:

Minitab17 from www.minitap.com

2.6.3. MOE (Molecular Operating Environment)

(MOE 2009.10 i4w9)

2.6.4. Software Methods

2.6.4.1. General method of ACD/lab program (Molecular Modelling)

There were two modes to ACD/ChemSketch, namely Structure and Draw. Structure mode was used to draw chemical molecules, while Draw mode used to create and edit graphical objects. Upon startup, the Draw Normal mode and Carbon were automatically selected. By clicking and dragging the cursor in the window, C-C bonds were created. Clicking on a carbon atom produces a branched structure. The change was made by selecting a heteroatom from the element list in the left toolbar and clicking on an atom in the structure to replace it. Radicals were made by selecting it from table which including carbon rings, carbon-based side chains and functional groups. A reaction requires were drawing by using the reaction arrow and reaction plus icons. Bond lengths and bond angle standardized by clicking on Clean Structure. The calculated properties were inserted into the ChemSketch window as a text field; on the tools menu, point to calculate, and choose the desired property. By selecting a structure and clicking on generate Name for structure, the IUPAC name was generated as a text field underneath the structure (Tables No [2.2.1] and [2.2.2]).

2.6.4.2. General method of Minitab to performed linear regression:

We use Minitab to perform a multiple linear regression analysis to get the equation which I can use to predict the biological activity

Minitab Procedures

Select Stat >> Regression >> Regression >> Fit Regression Model

Specify the response and the predictor(s). (For standard residual plots) Under Graphs..., select the desired residual plots. Minitab automatically recognizes replicates of data and produces Lack of Fit test with Pure error by default. Select OK.

Next, back up to the Main Menu having just run this regression:

(To get a prediction interval) Select Stat >> Regression >> Regression >> Predict ... Specify the response. Specify either the x value ("Enter individual values") or a column name ("Enter columns of values") containing multiplex values. Select Options... Specify the Confidence level — the default is 95%. Select OK. Select OK. The output will be displayed in the session window.

2.6.4.3. General Methods of MOE to Perform Docking

Protein Preparation: Three-dimensional coordinates (PDB code 4o6w) which affected HepG2 cells were downloaded from Protein Data Bank. The PDB file was submitted to MOE program and "Prepare PDB file for docking program" modules where missing side chains were modelled in, a small regularization was performed, water positions were corrected and hydrogen were added. Thus the water molecules and non-standard residues were removed.

Ligands Preparation: All the molecules were constructed with ACD/lab program and these geometries were optimized using the also ACD/lab to the corresponding mol2000 file that was submitted to MOE for PDB file preparation and docking with MOE 2009.10 The energy of built compound was minimized, slope of the logarithm of the molecule's partition coefficient between 1-octanol and water (SlogP-VSA8), slope of the molar refractivity (SMR-VSA2) and reflective of index were also calculated and saved as mol2000 files that was used in MOE.

Ligands Docking:

MOE 2009.10 was employed for docking simulations. The MOE program is a docking program was used to dock compounds on the active sites of protein 4o6w. For each compound the most stable docking model was selected according to the best scored conformation predicted. The complexes were energy minimized 1 force field till the gradient convergence 0.01kcal/mol was reached. Then the receptor–ligand interaction was saved as a JPG.

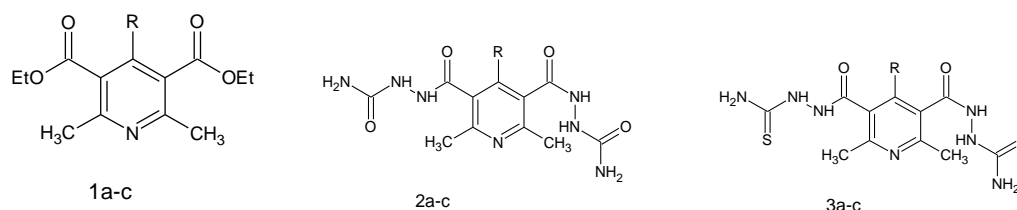
2.7. ACD Lab Method

A series of 40 compounds were designed by ACD Lab and their descriptors were calculated

2.8. QSAR Method

(Kumar *et al*, 2011) were studied anti-cancer activity of some new series of 1,4 dihydropyridine derivatives as showed in the table (2.1), their compounds were designed by ACD Lab and descriptor were calculated. The mathematical formula which related biological activity with structure (physicochemical parameter) was obtained by using MINITAB17 to performing multiple linear regressions by choosing randomly three descriptors as independent variable and plotted against biological activity as dependent variable.

Table (2.1) anti-cancer HepG2 (liver), activity of synthesised compounds by (Kumar, *et al*, 2011)



COMPOUND NO	R	TGI
1a	4-OH-3-OCH ₃ -Ph	29.1
1b	4-OH-Ph	25.2
1c	4-OCH ₃ -Ph	30.2
2a	4-OH-3-OCH ₃ -Ph	62.5
2b	4-OH-Ph	57.8
2c	4-OCH ₃ -Ph	54.1
3a	4-OH-3-OCH ₃ -Ph	47.8
3b	4-OH-Ph	51.2
3c	4-OCH ₃ -Ph	56.5

TGI= Tumour growth inhibitor

From above data QSAR obtained by selecting descriptors from ACD Lab and performing multiple linear regression by using MINITAB17.

2.9. Docking Method

In docking we need to place molecules in appropriate configuration to interact with receptor, in this study synthesized molecules placed in receptor 4o6w which affected Hep2 cell causing liver cancer.

2.10. Synthetic Methods

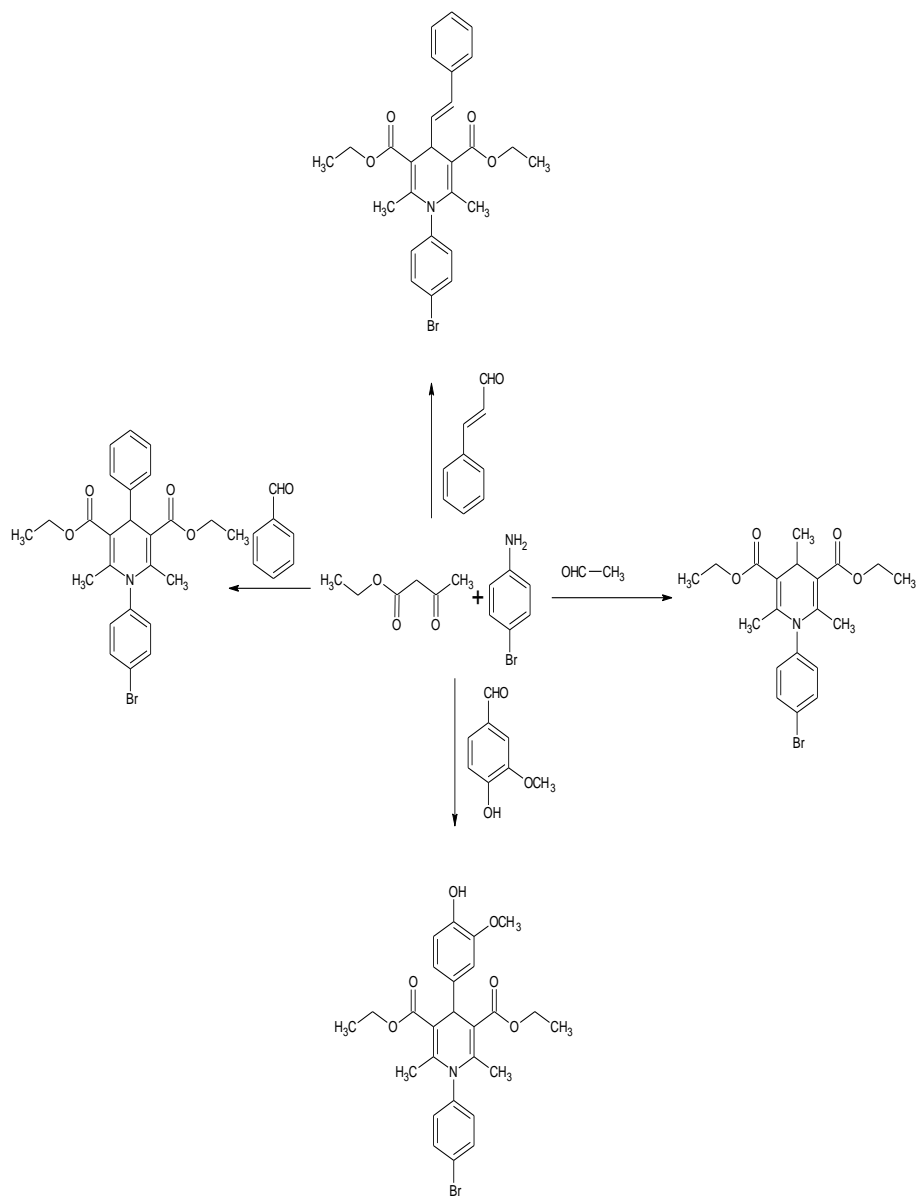
2.10.1 Preparation of Compound Ia-IVa (1,4-dihydro-2,6-dimethyl-4-alkyl pyridine-3,5-dicarboxylic acid diethyl ester)

To a solution of 0.3 mole aldehyde and 5ml of ethanol ethyl aceto acetate 7.6ml (0.6mole) and ammonium acetate 2.3g (0.3 moles) were added. The mixture was refluxed for four hours then the solid was collected and filtered. It was washed with cold ethanol and recrystallized from ethanol.

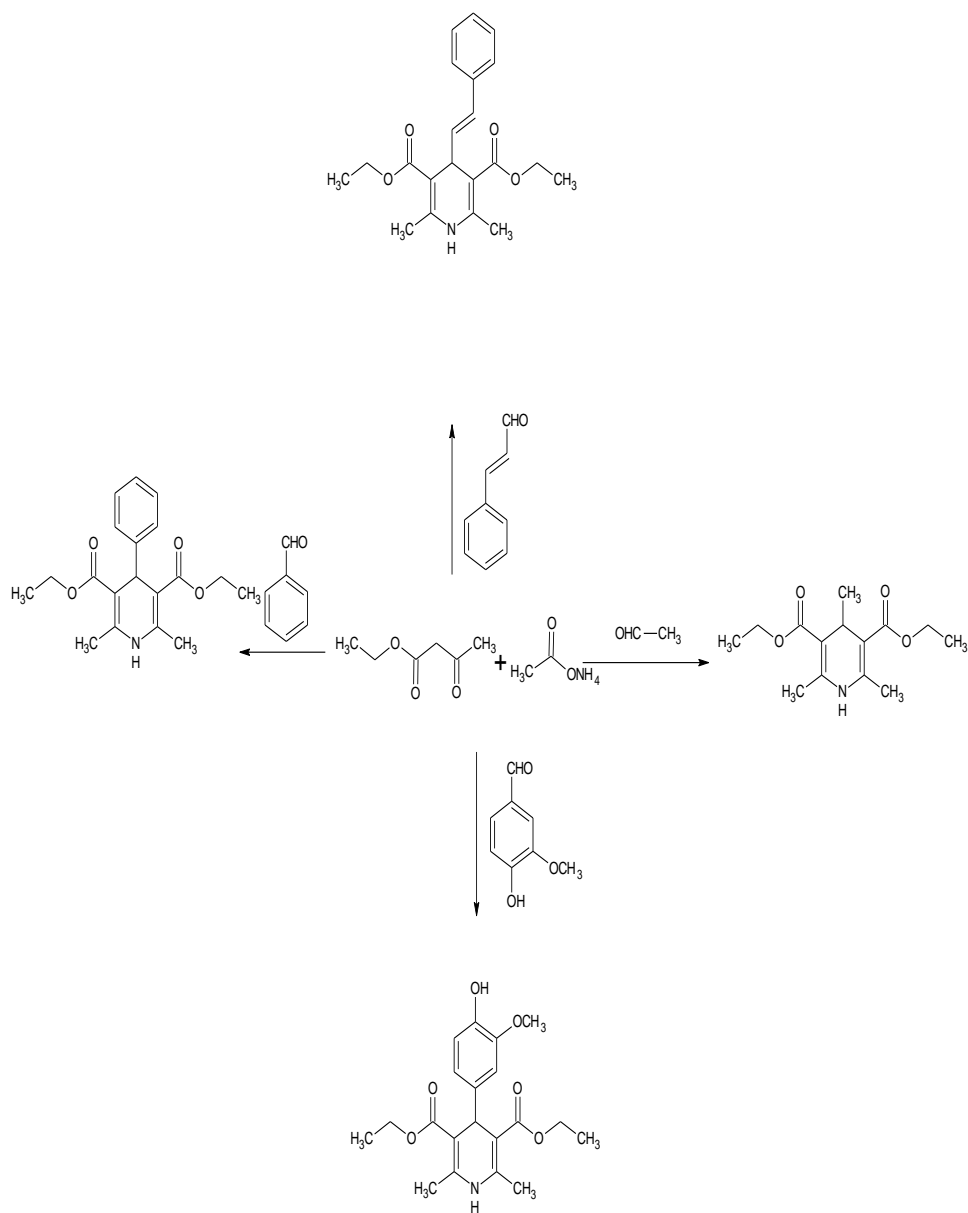
2.10.2 Preparation of compound Ib-IVb (N-bromophenyl 1,4-dihydro-2,6-dimethyl-4-methyl pyridine-3,5-dicarboxylic acid diethyl ester)

To a solution of 0.3moles aldehyde and 5ml of ethanol ethyl aceto acetate 7.6ml (0.6mole) and p-bromo aniline 5.2g (0.3 moles) were added. The mixture was refluxed for four hours then the solid was collected and filtered. It was washed with cold ethanol and recrystallized from ethanol.

2.11. Reaction Schemes



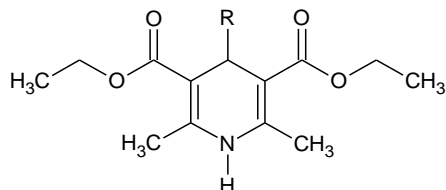
Scheme 2.1 Synthesis of N-bromophenyl 1,4-dihydro-2,6-dimethyl-4-alkylpyridine-3,5-dicarboxylic acid diethyl ester derivatives



Scheme 2.2 Synthesis 1,4dihydro-2,6dimethyl-4-alkayl pyridine-3,5- dicarboxylic acid diethyl ester derivatives

Table (2.2) Chemical names of the synthesized compounds

Chemical name of the synthesized 1,4dihydro-2,6dimethyl-4-alkayl pyridine-3,5-dicarboxylic acid diethyl ester



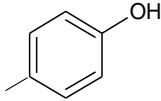
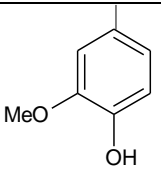
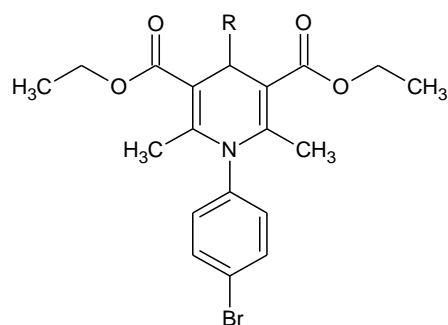
Compound No	R	Chemical Name
I	CH ₃	1,4dihydro-2,6dimethyl-4-methyl pyridine-3,5- dicarboxylic acid diethyl ester
II		1,4dihydro-2,6dimethyl-4-(phenyl) pyridine-3,5- dicarboxylic acid diethyl ester
III		1,4dihydro-2,6dimethyl-4-(hydroxyphenyl) pyridine-3,5- dicarboxylic acid diethyl ester
IV		1,4dihydro-2,6dimethyl-4-(4-hydroxy3-methoxyphenyl) pyridine-3,5- dicarboxylic acid diethyl ester

Table (2.3) Chemical name of the synthesized N-bromophenyl 1,4dihydro-2,6dimethyl-4-alkayl pyridine-3,5- dicarboxylic acid diethyl ester



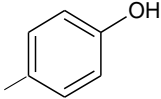
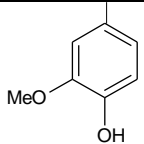
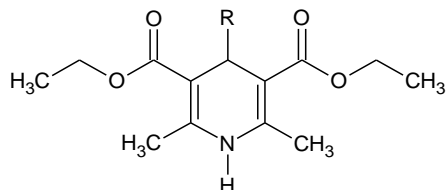
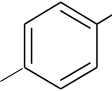
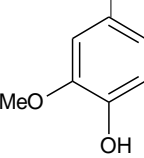
Compound No	R	Chemical Name
V	CH ₃	N-bromophenyl 1,4dihydro-2,6dimethyl-4-methyl pyridine-3,5-dicarboxylic acid diethyl ester
VI		N-bromophenyl 1,4dihydro-2,6dimethyl-4-phenyl pyridine-3,5-dicarboxylic acid diethyl ester
VII		N-bromophenyl -1,4dihydro-2,6dimethyl-4-(hydroxyphenyl) pyridine-3,5- dicarboxylic acid diethyl ester
VIII		N-bromophenyl -1,4dihydro-2,6dimethyl-4-(4-hydroxy3-methoxyphenyl) pyridine-3,5- dicarboxylic acid diethyl ester

Table (2.4) Reaction conditions of synthesized compounds

Reaction conditions of the synthesized 1,4dihydro-2,6dimethyl-4-alkayl pyridine-3,5- dicarboxylic acid diethyl ester



Comp. No	R	Solvent	Re. Time	Re. Temp.	Y%	Recrystallize solvent	m.p ^o c	M.wt g/mol
I	CH ₃	Ethanol	4hours	Reflux temperature	76%	Ethanol	175-178	253.298
II		Ethanol	4hours	Reflux temperature	61%	Ethanol	168-170	331.345
III		Ethanol/diethyl ether	4hours	Reflux temperature	53%	Ethanol	148-151	348.453
IV		Ethanol	4hours	Reflux temperature	88%	Ethanol	252-256	379.493

M.wt = molecular weight

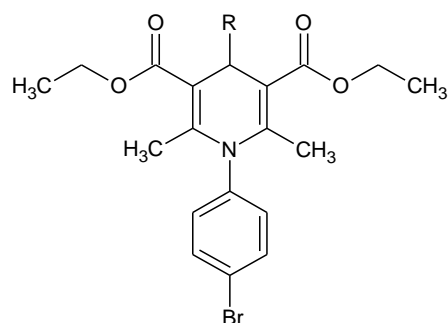
m.p = melting point

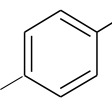
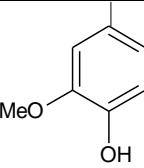
Re. Time = reaction time

Y% = Yield percentage

Re. Temp = reaction temperature

Table (2.5) Reaction conditions of the synthesized N-bromophenyl 1,4dihydro-2,6 dimethyl-4-alkayl pyridine-3,5- dicarboxylic acid diethyl ester



Comp. No	R	Solvent	Re. Time	Re. Temp.	Y%	Recrystallize solvent	m.p ⁰ c	M.wt
V	CH ₃	Ethanol	4hours	Reflux temperature	25%	Ethanol	170-174	410.298
VI		Ethanol	4hours	Reflux temperature	83%	Ethanol	152-156	472.369
VII		Ethanol/di ethyl ether	4hours	Reflux temperature	56%	Ethanol	204-206	456.377
VIII		Ethanol	4hours	Reflux temperature	84%	Ethanol	211--214	486.417

M.wt = molecular weight

m.p = melting point

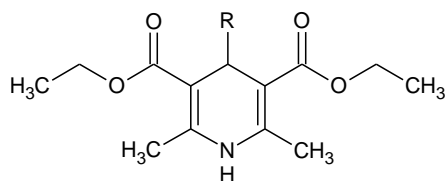
Re. Time = reaction time

Y% = Yield percentage

Re. Temp = reaction temperature

Table (2.6) Thin layer chromatography of the synthesized compound

Thin layer chromatography of the synthesized 1,4dihydrop-2,6dimethyl-4-alkayl pyridine-3,5- dicarboxylic acid diethyl ester



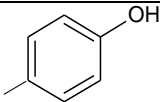
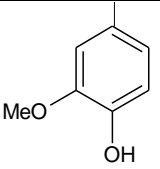
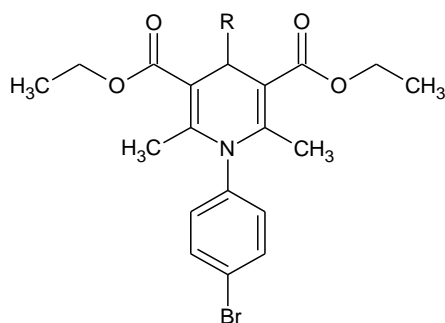
Comp. No	R	Developing Solvent	R _f
I	CH ₃	Water/ethanol(2:8)	0.56
II		Water/ethanol(2:8)	0.43
III		Water/ethanol(2:8)	0.66
IV		Water/ethanol(2:8)	0.79

Table (2.7) Thin layer chromatography of the synthesized N-bromophenyl 1,4-dihydro-2,6-dimethyl-4-alkyl pyridine-3,5-dicarboxylic acid diethyl ester



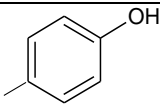
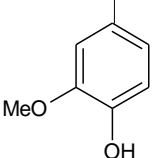
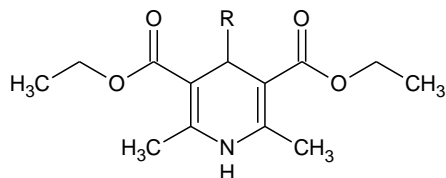
Comp. No	R	Developing solvent	R _f
V	CH ₃	Water/ethanol(2:8)	0.48
VI		Water/ethanol(2:8)	0.23
VII		Water/ethanol(2:8)	0.60
VIII		Water/ethanol(2:8)	0.71

Table (2.8) thin layer chromatography of compounds which used to preparation of synthesized compounds

Comp. name	Developing solvent	R_f
Ethyl aceto acetate	Water/ethanol(2:8)	0.78
Ammonium acetate	Water/ethanol(2:8)	0.88
p-bromo aniline	Water/ethanol(2:8)	0.70
Acetaldehyde	Water/ethanol(2:8)	0.81
Benzaldehyde	Water/ethanol(2:8)	0.39
Salicylaldehyde	Water/ethanol(2:8)	0.42
Vanillin	Water/ethanol(2:8)	0.50

Table (2.9) Infrared spectral data of the synthesized compounds

Infrared spectral data of the synthesized 1,4-dihydro-2,6-dimethyl-4-alkyl pyridine-3,5-dicarboxylic acid diethyl ester



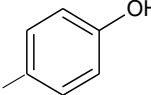
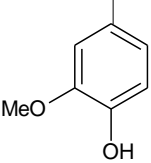
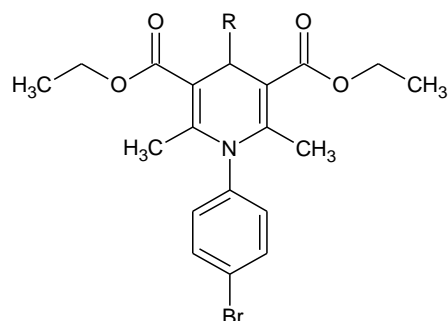
Comp No	R	C=O st.vib	N-H st.vib	C=C st.vib	C-H st.vib	C-O st.vib	OH st.vib
I	CH ₃	1700	3250	1300-1370-1500-1630	2990	1220	-
II		1690	3300	1450-1500-1600-1650	2980	1210	-
III		1740	3250	1460-1500-1550-1610	2900	1220	3200-3600
IV		1700	3310	1410-1460-1520-1610	2985	1200	3100-3420

Table (2.10) Infrared spectral data of the synthesized synthesized N-bromophenyl 1,4-dihydro-2,6-dimethyl-4-alkyl pyridine-3,5-dicarboxylic acid diethyl ester



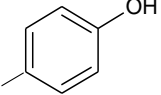
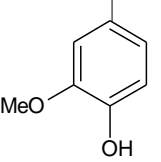
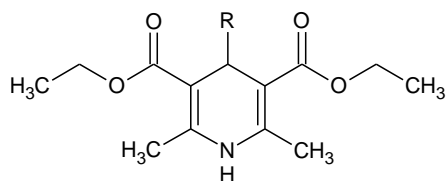
Comp No	R	C-H st.vib	C=O st.vib	$\text{C}=\text{C}$ st.vib	C-H st.vib	N-H st.vib	C-O st.vib	OH st.vib
V	CH ₃	2920	1720		2990	-	1200	-
VI		2990	1700	1350-1400-1510-1590	2850	-	1235	-
VII		2900	1710	1400-1450-1520-1610	2900	-	1225	3210-3400
VIII		2980	1690	1380-1420-1520-11600	2950	-	1210	35210

Table (2.11) Infrared spectral data of compounds which used to preparation of synthesized compounds

Comp. name	C=O st.vib	$\text{C} \equiv \text{C}$ st.vib	C-H st.vib	OH st.vib	C-O st.vib
Ethyl acetoacetate	1745-1725	-	2990	-	1240
p-bromo aniline	-	1450-1500-1540-1610	2980	3300-3400	
Acetaldehyde	1725	-	2900	-	1350
Benzaldehyde	1705	1390-1450 1580 1620	2860	-	1205
Salicylaldehyde	1665	1460-1487-1581-1595	2847	3200	1220
Vanillin	1720	1465-1510-1590-1650	2950	3170	1260

Table (2.12) ultra violet- visible spectral data of the synthesized compounds

ultra violet- visible spectral data of the synthesized 1,4dihydro-2,6dimethyl-4-alkayl pyridine-3,5- dicarboxylic acid diethyl ester



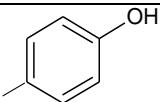
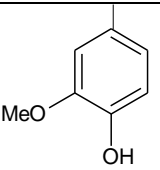
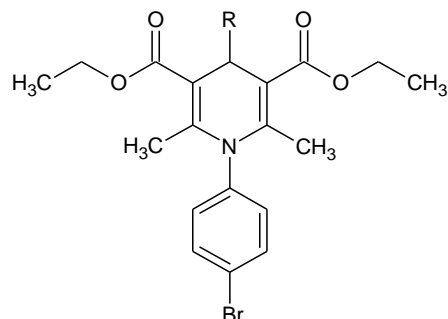
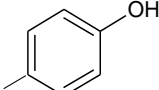
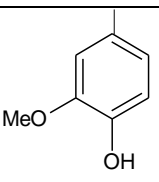
Comp. No	R	Solvent	λ_{\max} nm
I	CH ₃	Methanol	346
II		Methanol	322
III		Methanol	298
IV		Methanol	349

Table (2.13) ultra violet- visible spectral data of the synthesized synthesized N-bromophenyl 1,4dihydro-2,6dimethyl-4-alkayl pyridine-3,5- dicarboxylic acid diethyl ester



Comp. No	R	Solvent	λ_{\max} nm
V	CH ₃	Methanol	316
VI		Methanol	313
VII		Methanol	340
VIII		Methanol	326

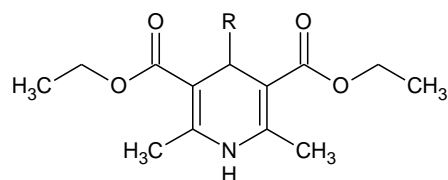
3. Results and Discussion

1,4-DHP derivatives are large group of structurally diverse compounds with a broad range of pharmacological activities. Introduction and variation of the substituents at the 1,4-DHP ring can result in elaboration of the compounds which can be capable to interact at diverse receptors and ion channels. In the same way these activities depend on various structural parameters related to DHPs (presence and character of substituents), lipophilicity, and depth of the incorporation in the biological membranes. Additionally, the main structure element – the DHP cycle – can be regarded as a model of the redox coenzyme NAD(P)H or as analogue of 1,4-dihydronicotinic amide. 1,4-Dihydropyridines regulate redox reactions, possess free radical-scavenging properties, inhibit the peroxidation processes and protect biological membranes (Klusa 2016). The early prediction of activity related characteristics of drug candidates is an important problem in drug design. A large ratio of the capital spent while commercializing a drug is spent on unsuccessful candidate drugs. Therefore, eliminating molecules with undesired properties beforehand has been one of the central research subjects in structure based drug design. Since the number of possible drug candidates is often in the order of millions, computerized methods are used for prediction of activities. One way is to study chemical structures of the candidate molecules and to predict the activity levels of drug candidates based on them. One of the data driven methods that is widely used in drug design is QSAR (quantitative structure-activity relationship). QSAR is the effort of understanding correlation between the chemical structure of a molecule and its biological and chemical activities such as biotransformation ability, reaction ability, solubility or target activity. The main assumption in QSAR is that structurally similar molecules tend to have similar activities and that molecules with unknown properties can be compared to structures with known properties. 3D structures of molecules may be used to find many candidate molecules that will fit into the target binding site, which can be constructed using a variety of methods. The problem of early prediction of properties of drug candidates becomes a machine learning problem when there are a number of structurally similar molecules of known activities that fit into the binding site. The activity of the molecules is usually classified into two classes: high or low active based on their toxicity. The reason for this binary classification is that the numerical values for biological activities are not available in most cases.

ACD/ChemSketch Freeware was used to draw chemical structures, calculation of molecular properties molecular weight, density, molar volume, polarizability, parachor, Index of Refraction, naming structures and prediction of log P.

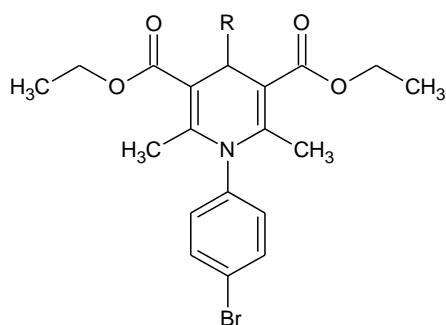
3.1. ACD/Lab results

Table No. (3.1) ACD/Lab results of the synthesized 1,4dihydro-2,6dimethyl-4-alkyl pyridine-3,5- dicarboxylic acid diethyl ester



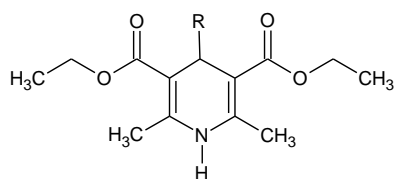
Co.No	R	Log P	Molar volume ±3.0cm ³	Density ±0.06g/cm ³	Polarizability ±0.5 10- 24cm ³	Parachor ± 6.0 cm ³	Index of Refraction ± 0.02
I	CH ₃	3.01	249.2	1.072	28.10	598.7	1.480
II		4.30	293.4	1.122	35.92	732.5	1.529
III		3.56	291.8	1.183	36.67	747.7	1.546
IV		3.27	315.8	1.188	39.32	806.3	1.540

Table No. (3.2) ACD/Lab results of the synthesized N-bromophenyl 1,4dihydro-2,6dimethyl-4-alkayl pyridine-3,5- dicarboxylic acid diethyl ester



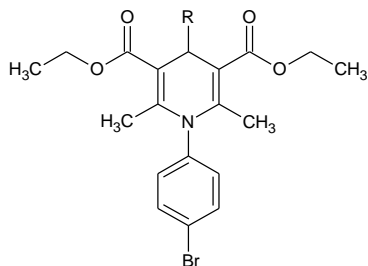
Co.No	R	Log P	Molar volume ±3.0cm ³	Density ±0.06g/cm ³	Polarizability ±0.5 10- 24cm ³	Parachor ± 6.0 cm ³	Index of Refraction ± 0.02
V	CH ₃	4.05	324.6	1.300	40.92	821.7	1.548
VI		5.52	368.8	1.313	48.75	955.5	1.581
VII		4.78	367.2	1.362	49.49	970.7	1.595
VIII		4.49	391.2	1.355	52.14	1029.3	1.587

Table No. (3.3) ACD/Lab results of some 1,4-dihydro-2,6-dimethyl-4-alkyl pyridine-3,5-dicarboxylic acid diethyl ester



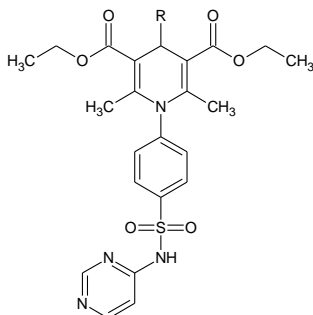
Co.No	R	Log P	Molar volume ±3.0cm ³	Density ±0.06g/cm ³	Polarizability ±0.5 10- 24cm ³	Parachor ± 6.0 cm ³	Index of Refraction ± 0.02
IX	H	2.51	229.2	1.104	26.23	560.7	1.489
X		3.46	276.2	1.156	32.87	687.7	1.512
XI		3.98	282.9	1.185	35.28	717.4	1.541
XII		4.91	307.3	1.156	41.00	800.3	1.587
XIII		3.89	281.3	1.049	31.73	676.8	1.480
XIV		5.07	309.6	1.318	38.97	783.6	1.547

Table No. (3.4) ACD/Lab results of some N-bromo phenyl 1,4dihydro-2,6dimethyl-4-alkayl pyridine-3,5- dicarboxylic acid diethyl ester



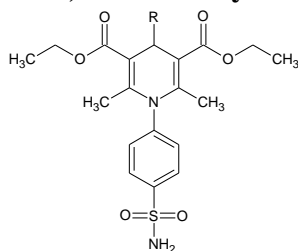
Co.No	R	Log P	Molar volume ±3.0cm ³	Density ±0.06g/cm ³	Polarizability ±0.5 10- 24cm ³	Parachor ± 6.0 cm ³	Index of Refraction ± 0.02
XV	H	3.56	304.6	1.340	39.06	783.7	1.560
XVI		4.68	351.6	1.348	45.69	910.7	1.569
XVII		5.19	358.3	1.368	48.11	940.4	1.592
XVIII		5.92	382.7	1.333	53.82	1023.2	1.627
XIX		4.93	356.7	1.262	44.55	899.8	1.542
XX		6.29	385.0	1.462	51.80	1006.5	1.594

Table No. (3.5) ACD/Lab results of some N-(pyrimidin-4-yl)benzene sulfonamido 1,4-dihydro-2,6-dimethyl-4-alkyl pyridine-3,5-dicarboxylic acid diethyl ester



Co.No	R	Log P	Molar volume ±3.0cm ³	Density ±0.06g/cm ³	Polarizability ±0.5 10- 24cm ³	Parachor ± 6.0 cm ³	Index of Refraction ± 0.02
XXI	H	0.05	364.0	1.336	49.23	1003.7	1.597
XXII	CH ₃	0.55	384.0	1.303	51.05	1041.7	1.585
XXIII		2.01	428.2	1.313	59.01	1175.5	1.612
XXIV		1.28	426.6	1.356	59.62	1190.7	1.622
XXV		0.98	450.6	1.350	62.14	1249.4	1.612
XXVI		1.18	411.0	1.344	56.03	1130.7	1.603
XXVII		1.69	417.7	1.361	58.28	1160.4	1.621
XXVIII		2.93	460.6	1.308	64.49	1283.3	1.624
XXIX		1.42	416.1	1.270	54.71	1119.8	1.577
XXX		2.79	444.4	1.443	62.07	1226.6	1.622

Table No. (3.6) ACD/Lab results of some N-benzene sulphonamide 1,4-dihydro-2,6-dimethyl-4-alkyl pyridine-3,5-dicarboxylic acid diethyl ester



Co.No	R	Log P	Molar volume ±3.0cm ³	Density ±0.06g/cm ³	Polarizability ±0.5 10- 24cm ³	Parachor ± 6.0 cm ³	Index of Refraction ± 0.02
XXXI	H	0.89	317.4	1.286	41.16	840.2	1.568
XXXII	CH ₃	1.38	337.4	1.252	42.99	878.3	1.555
XXXIII		2.85	381.6	1.269	50.95	1012.1	1.588
XXXIV		2.12	380.0	1.317	51.56	1027.3	1.600
XXXV		1.82	404.0	1.313	54.08	1085.9	1.590
XXXVI		2.01	364.4	1.302	47.97	967.3	1.578
XXXVII		2.53	371.0	1.322	50.21	996.9	1.598
XXXVIII		3.25	395.5	1.290	54.59	1079.8	1.613
XXXIX		2.26	369.5	1.219	46.65	956.4	1.549
XL		3.62	397.7	1.416	54.01	1063.1	1.600

3.2. QSAR Results

Data reported by kumar, table (2.1), their compounds were designed by using ACD Lab and the descriptors were calculated. Minitab were used to performed a multiple linear regression to obtained QSAR equation.

A number of equations were obtained the best of them were

$$1- \text{LogTGI} = 3.00 + 2.200 \text{ Density} + 0.00610 \text{ molar refractivity} - 3.07 \text{ indext of refraction} + 0.0016 \text{ Log P}$$

$$\text{With } R^2 = 0.9567$$

$$2- \text{Log TGI} = 0.03 + 1.288 \text{ Density} - 0.00064 \text{ molar volume} + 0.0132 \text{ LogP}$$

$$\text{With } R^2 = 0.8675$$

$$3- -\text{LogGI50} = -1.88 + 2.63 \text{ Density} - 0.0039 \text{ molar refractivity} + 0.037 \text{ LogP}$$

$$\text{With } R^2 = 0.3068$$

$$4- \text{LogGI50} = 4.09 + 0.222 \text{ Density} + 0.00228 \text{ molar refractivity}$$

$$+ 1.73 \text{ indext of refraction} - 0.0940 \text{ Log P}$$

$$\text{With } R^2 = 0.5525$$

$$5- -\text{logGI50} = -1.88 + 0.037 \text{ Log P} - 0.0039 \text{ molar refractivity} + 2.63 \text{ Density}$$

$$\text{With } R^2 = 0.2155$$

$$6- \text{log IC50} = 2.32 - 0.550 \text{ Density} + 0.00317 \text{ molar refractivity}$$

$$+ 0.04 \text{ indext of refraction} - 0.0243 \text{ Log P}$$

$$\text{With } R^2 = 0.4401$$

$$7- \text{log P TGI} = 3.00 + 2.200 \text{ Density} + 0.00610 \text{ molar refractivity} -$$

$$3.07 \text{ indext of refraction} + 0.0016 \text{ Log P}$$

$$\text{With } R^2 = 0.9134$$

Equation umber 2 was used to predict biological activities of designed compounds.

Table (3.7) and (3.8) showed) descriptors which used to performing Multiple Linear Regression to obtaining QSAR equation

Table No (3.7) descriptors which used to performing Multiple Linear Regression to obtaining QSAR equation

$$\text{Log TGI} = -0.03 + 1.288 \text{ Density} - 0.00064 \text{ molar volume} + 0.0132 \text{ LogP}$$

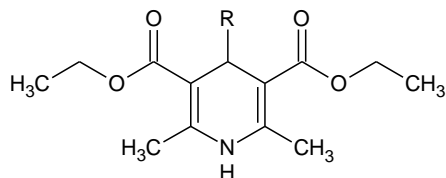
COMPOUND NO	logTGI	Density	molar volume	LogP
1a	1.463	1.188	229.2	3.27
1b	1.401	1.183	249.2	3.56
1c	1.480	1.132	293.4	4.21
2a	1.795	1.411	291.8	1.68
2b	1.761	1.425	315.8	1.39
2c	1.733	1.352	276.2	0.73
3a	1.679	1.386	282.9	0.47
3b	1.709	1.457	307.3	0.18
3c	1.752	1.442	281.3	0.47

Table No (3.8) descriptors which used to performing Multiple Linear Regression to obtaining QSAR equation

$$\text{LogTGI} = 3.00 + 2.200 \text{ D} + 0.00610 \text{ M volume} + 3.07 \text{ index re} + 0.0016 \text{ LoP}$$

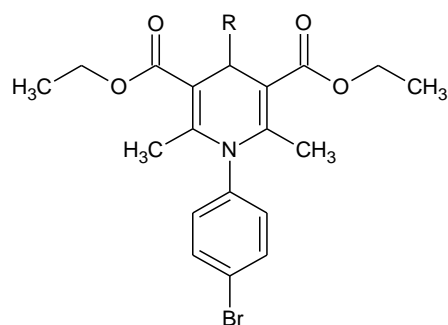
Comp No	LogTGI	Density	molar volume	index of refraction
1a	1.463	1.188	229.2	1.540
1b	1.401	1.183	249.2	1.546
1c	1.480	1.132	293.4	1.525
2a	1.795	1.411	291.8	1.620
2b	1.761	1.425	315.8	1.634
2c	1.733	1.352	276.2	1.603
3a	1.679	1.386	282.9	1.665
3b	1.709	1.457	307.3	1.702
3c	1.752	1.442	281.3	1.683

Table No. (3.9) QSAR results of the synthesized 1,4dihydro-2,6dimethyl-4-alkayl pyridine-3,5- dicarboxylic acid diethyl ester



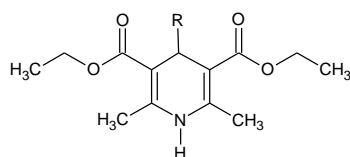
Co.No	R	Log P	Molar volume ±3.0cm ³	Density ±0.06g/cm ³	Log TGI	Predicted biological activity (TGI)
I	CH ₃	3.01	249.2	1.072	1.2307	17.00
II		4.30	293.4	1.122	1.2856	19.30
III		3.56	291.8	1.183	1.3539	22.58
IV		3.27	315.8	1.188	1.3411	21.92

Table No. (3.10) QSAR results of the synthesized N-bromophenyl 1,4-dihydro-2,6-dimethyl-4-alkyl pyridine-3,5-dicarboxylic acid diethyl ester



Co.No	R	Log P	Molar volume ±3.0cm ³	Density ±0.06g/cm ³	Log TGI	Predicted biological activity (TGI)
V	CH ₃	4.05	324.6	1.300	1.4906	30.90
VI		5.52	368.8	1.313	1.497	29.51
VII		4.78	367.2	1.362	1.552	35.48
VIII		4.49	391.2	1.355	1.5242	33.11

Table No. (3.11) QSAR results of some 1,4dihydro-2,6dimethyl-4-alkayl pyridine-3,5- dicarboxylic acid diethyl ester

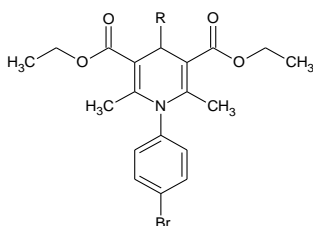


By using equation No(2)

$$\text{Log TGI} = -0.03 + 1.288 \text{ Density} - 0.00064 \text{ molar volume} + 0.0132 \text{ LogP}$$

Co.No	R	Log P	Molar volume ±3.0cm ³	Density ±0.06g/cm ³	Log TGI	Predicted biological activity (TGI)
IX	H	2.51	229.2	1.104	1.5151	32.74
X		3.46	276.2	1.156	1.3276	21.23
XI		3.98	282.9	1.185	1.3675	23.28
XII		4.91	307.3	1.156	2.0864	120.22
XIII		3.89	281.3	1.049	1.1923	15.48
XIV		5.07	309.6	1.318	1.5359	33.88

3.2.4. Table No. (3.12) QSAR results of some N-bromo phenyl 1,4dihydro-2,6dimethyl-4-alkayl pyridine-3,5- dicarboxylic acid diethyl ester

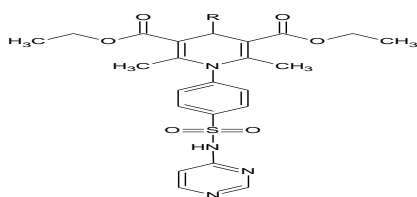


By using equation No (2)

$$\text{Log TGI} = -0.03 + 1.288 \text{ Density} - 0.00064 \text{ molar volume} + 0.0132 \text{ LogP}$$

Co.No	R	Log P	Molar volume ±3.0cm ³	Density ±0.06g/cm ³	Log TGI	Predicted biological activity (TGI)
XV	H	3.56	304.6	1.340	1.5479	35.23
XVI		4.68	351.6	1.348	1.5427	34.67
XVII		5.19	358.3	1.368	1.5705	37.15
XVIII		5.92	382.7	1.333	1.5201	33.10
XIX		4.93	356.7	1.262	1.4160	26.30
XX		6.29	385.0	1.462	1.6900	48.97

3.2.5. Table No. (3.13) QSAR results of some N-(pyrimidin-4-yl)benzene sulfonamido 1,4dihydro-2,6dimethyl-4-alkayl pyridine-3,5- dicarboxylic acid diethyl ester

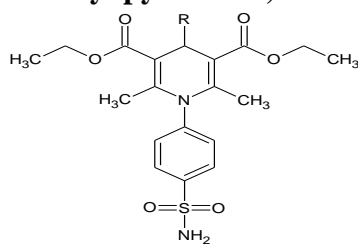


By using equation No (2)

$$\text{Log TGI} = -0.03 + 1.288 \text{ Density} - 0.00064 \text{ molar volume} + 0.0132 \text{ LogP}$$

Comp. No	R	Log P	Molar volume ±3.0cm ³	Density ±0.06g/cm ³	Log TGI	Predicted biological activity (TGI)
XXI	H	0.05	364.0	1.104	1.159	14.12
XXII	CH ₃	0.55	384.0	1.072	1.112	12.88
XXIII		2.01	428.2	1.122	1.167	14.45
XXIV		1.28	426.6	1.183	1.236	16.98
XXV		0.98	450.6	1.188	1.224	16.59
XXVI		1.18	411.0	1.156	1.210	16.21
XXVII		1.69	417.7	1.185	1.251	17.78
XXVIII		2.93	460.6	1.156	1.202	15.84
XXIX		1.42	416.1	1.049	1.073	11.75
XXX		2.79	444.4	1.318	1.419	25.70

3.2.6. Table No. (3.14) QSAR results of some N-benzene sulphonamido 1,4-dihydro-2,6-dimethyl-4-alkyl pyridine-3,5-dicarboxylic acid diethyl ester



By using equation No (2)

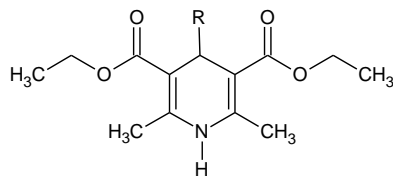
$$\text{Log TGI} = -0.03 + 1.288 \text{ Density} - 0.00064 \text{ molar volume} + 0.0132 \text{ LogP}$$

Comp. No	R	Log P	Molar volume ±3.0cm ³	Density ±0.06g/cm ³	Log TGI	Predicted biological activity (TGI)
XXXI	H	0.89	317.4	1.286	1.4347	26.91
XXXII	CH ₃	1.38	337.4	1.252	1.3852	23.98
XXXIII		2.85	381.6	1.269	1.3976	24.55
XXXIV		2.12	380.0	1.317	1.4509	28.18
XXXV		1.82	404.0	1.313	1.4270	26.30
XXXVI		2.01	364.4	1.302	1.4395	26.91
XXXVII		2.53	371.0	1.322	1.4683	28.84
XXXVIII		3.25	395.5	1.290	1.4209	26.30
XXXIX		2.26	369.5	1.219	1.2598	17.78
XL		3.62	397.7	1.416	1.5867	38.01

3.3. Docking Result:

3.3.1 Docking scores

Table 3.15. Docking Scores of some 1,4-dihydro-2,6-dimethyl-4-alkyl pyridine-3,5-dicarboxylic acid diethyl ester



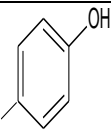
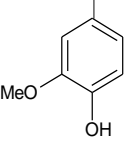
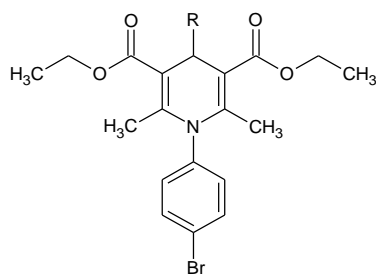
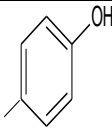
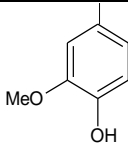
Comp. No	R	S	Amino acid interacted	Interacted group	Type of interaction
I	CH ₃	-14.9892	His538	Carbonyl group	Side chain acceptor
II		-18.0663	His538	Benzene ring	Arene - cation
III		-18.0998	His538	Carbonyl group	Side chain acceptor
IV		-16.8426	Gly494 Lys540 Arg557	Methoxy group Carbonyl group Benzene ring	Backbone acceptor Side chain acceptor Arene - cation

Table 3.16. Docking Scores of some N-bromo phenyl 1,4-dihydro-2,6-dimethyl-4-alkyl pyridine-3,5-dicarboxylic acid diethyl ester



Comp. No	R	S	Amino acid interacted	Interacted group	Type of interaction
V	CH ₃	-17.1734	-	-	-
VI		-19.3834	His538	Benzene ring	Arene - Arene
VII		-20.2331	His538	Benzene ring	Arene - cation
VIII		-20.1053	His538 Lys540	Benzene ring Methoxy group	Arene – Arene Backbone acceptor

Docking scores(S) is measure of binding affinity between the ligand and the receptor small value means higher affinity.

In this Research docking scores of the synthesized compounds were compared with standard Doxorubicin (familiar anti-cancer drug) which were docked against receptor 4o6w and (S) value were calculated (-21.6769).

After comparison synthesized compounds shows affinity approximately similar with standard specially compounds (VII and VIII).

3.3.2. Interaction between designed molecules and receptor 4o6w

Two molecules of high interaction and two molecules of low interaction were studied in below figures to describe interaction in Docking process.

Figure (3.1) interaction between compound 25 and receptor 4o6w

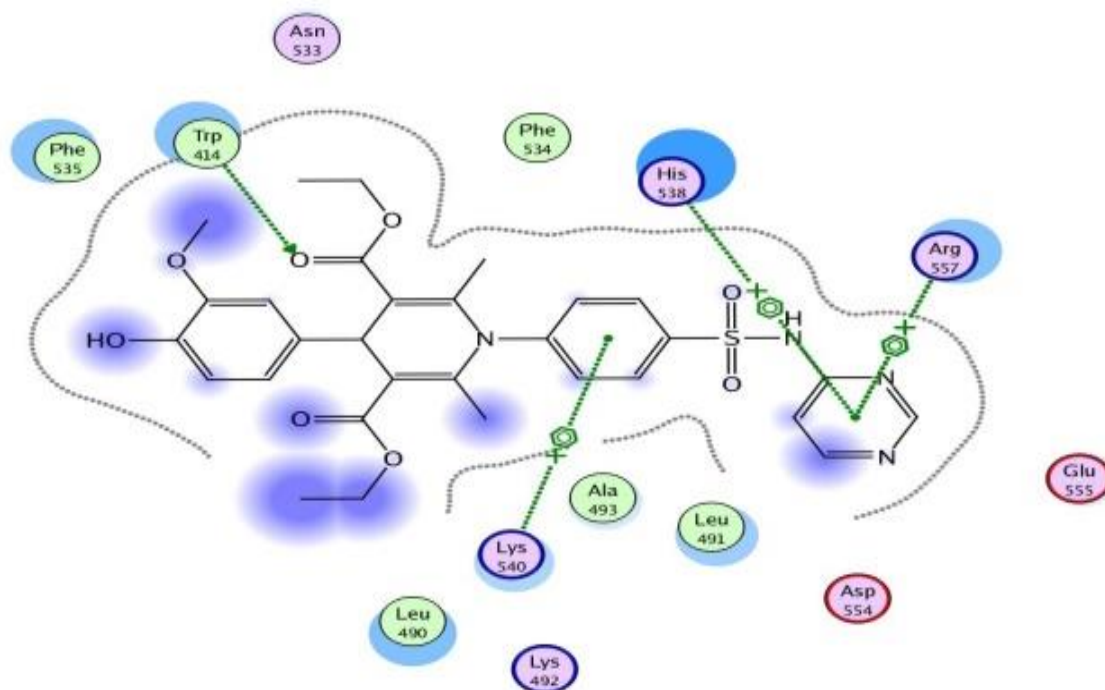


Figure (3.2) interaction between compound 35 and receptor 406w

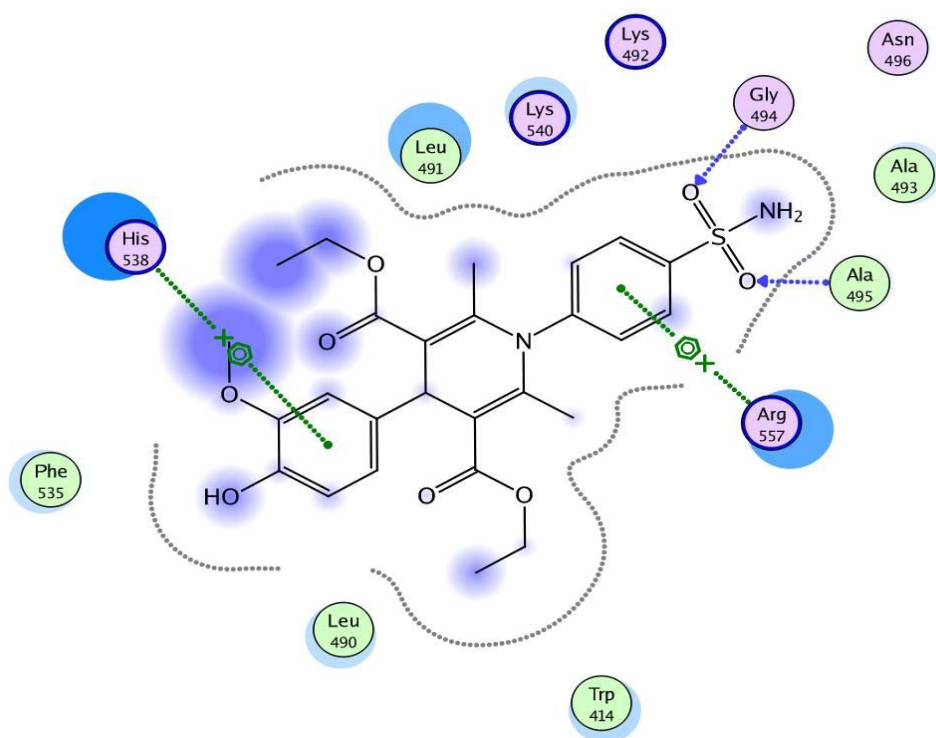


Figure (3.3) Interaction between compound 4 and receptor 406w

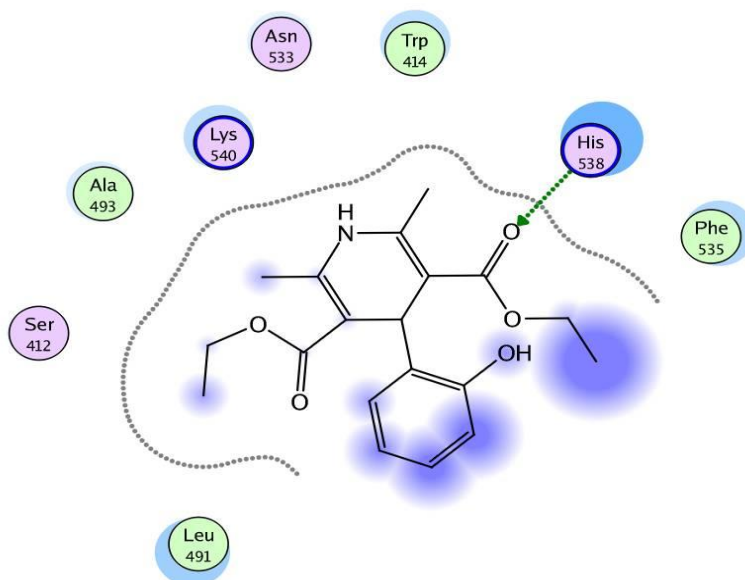


Figure (3.4) Interaction between compound 6 and receptor 4o6w

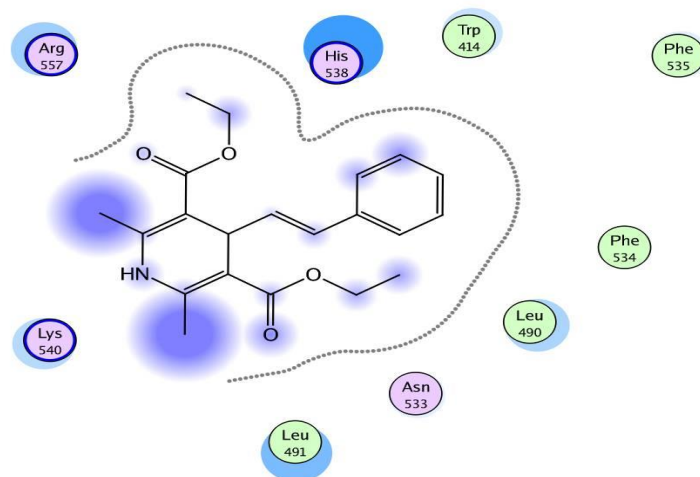
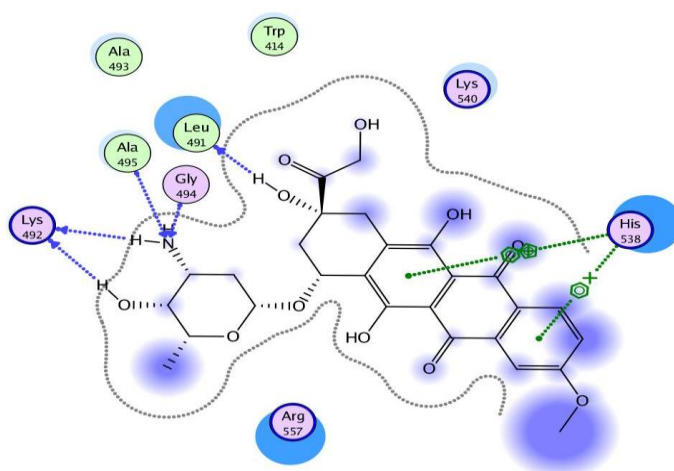


Figure (3.5) Interaction between standard doxorubicin and receptor 4o6w



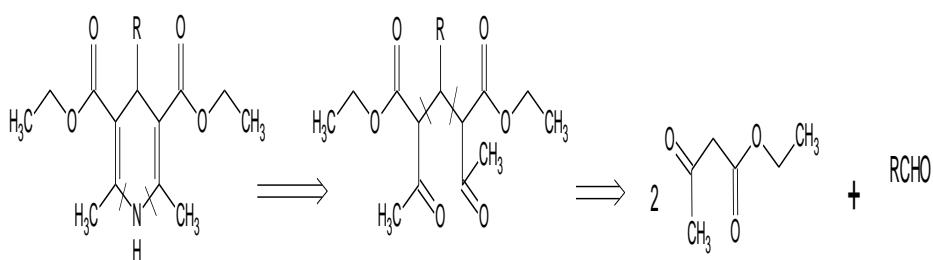
According to docking and QSAR studies compounds by taking in consideration R^2 value from the equation of QSAR , interaction of the molecules and the receptor in the Docking studies and docking scores values (2, 3, 4, 5, 12, 13, 14 and 15) were synthesized and characterized and called (I, II, III, IV, V, VI, VII and VIII) respectively .

The identity of the prepared compound was confirmed by spectral (IR, UV), chromatographic (TLC) and classical data (m.p, colour).

3.4. Analysis of 1,4dihydro-2,6dimethyl-4-alkayl pyridine-3,5- dicarboxylic acid diethyl ester

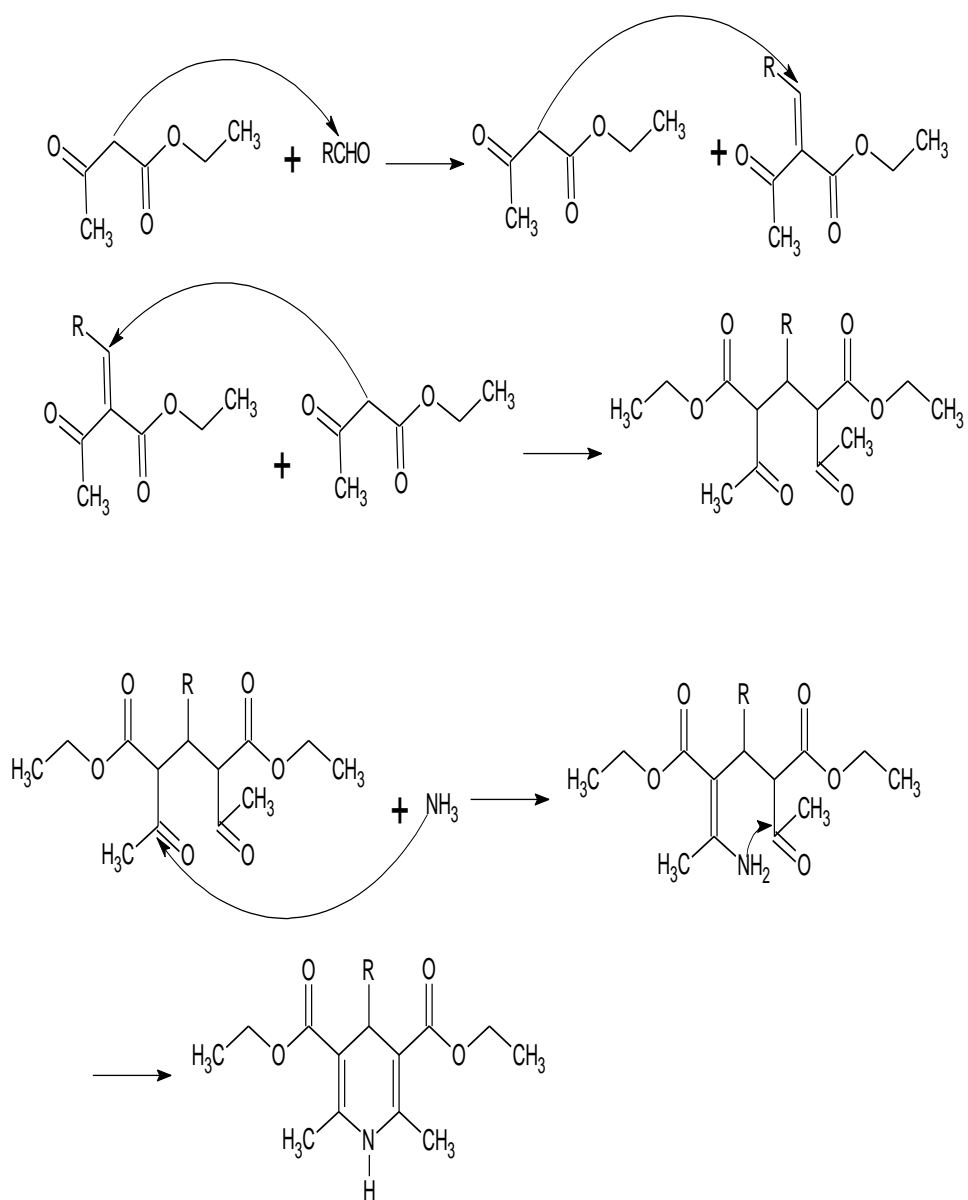
3.4.1. Retro-synthetic disconnection of 1,4dihydro-2,6dimethyl-4-alkayl pyridine-3,5- dicarboxylic acid diethyl ester

The synthetic designing of the 1,4dihydro-2,6dimethyl-4-alkayl pyridine-3,5-dicarboxylic acid diethyl ester in this work was adopted through the disconnection approach. The retro-synthetic analysis of these compounds can be shown below:



3.4.2. Mechanism of formation of 1,4dihydro-2,6dimethyl-4-alkayl pyridine-3,5- dicarboxylic acid diethyl ester

The reaction of 2:1 molar ratio of the required Ethyl aceto acetate and the aldehyde can produce the Ia product which reacted with ammonium acetate to give the final product. The mechanism of such reaction can be illustrated below:



(Kumar *et al*, 2011)

3.4.3. Spectral data of 1,4dihydropyridine

3.4.3.1. IR Spectral data of 1,4dihydro-2,6dimethyl-4-alkyl pyridine-3,5-dicarboxylic acid diethyl ester

The *IR* spectrum of synthesized compounds showed a characteristic bands of the carbonyl groups at (1700, 1690, 1740 and 1700) cm^{-1} for compounds (Ia, IIa, IIIa and IVa) respectively as expected.

The *IR* spectrum showed bands at 3150, 3300, 3250.3310 cm^{-1} for compounds (Ia, IIa, IIIa and IVa) respectively as indication of N-H stretching vibration of secondary aromatic amines.

The *IR* spectrum showed bands at 1300, 1370, 1500 and 1630 for compound Ia indicated $\text{C}=\text{C}$ stretching vibration for the aromatic ring.

The *IR* spectrum showed bands at 1450, 1500, 1600 and 1650 for compound IIa indicated $\text{C}=\text{C}$ stretching vibration for the aromatic ring.

The *IR* spectrum showed bands at 1460, 1500, 1550 and 1610 for compound IIIa indicated $\text{C}=\text{C}$ stretching vibration for the aromatic ring.

The *IR* spectrum showed bands at 1410, 1460, 1520 and 1610 for compound IVa indicated $\text{C}=\text{C}$ stretching vibration for the aromatic ring.

The *IR* spectrum showed bands at 1220, 1210, 1220 and 1200 cm^{-1} for compounds (I, II, III and IV) respectively as indication of C-O stretching vibration.

The *IR* spectrum showed bands at (3200-3600 and 3100-3420) cm^{-1} for compounds (III and IV) respectively as indication of O-H stretching vibration.

The *IR* spectrum showed bands at (2990, 2980, 2900 and 2985) cm^{-1} for compounds (III and IV) respectively as indication of C-H stretching vibration of the aliphatic part.

3.4.3.2. IR Spectral data of N-bromophenyl 1,4dihydro-2,6dimethyl-4-alkyl pyridine-3,5- dicarboxylic acid diethyl ester

The IR spectrum of synthesized compounds showed a characteristic bands of the carbonyl groups at (1720, 1700, 1710 and 1690) cm^{-1} for compounds (V, VI, VII and VIII) respectively as expected.

The IR spectrum showed no bands at area of N-H stretching vibrations as expected because there is no N-H group.

The IR spectrum showed bands at 1300, 1370, 1500 and 1630 for compound V indicated $\text{C}=\text{C}$ stretching vibration for the aromatic ring.

The IR spectrum showed bands at 1350, 1400, 1510 and 1590 for compound VI indicated $\text{C}=\text{C}$ stretching vibration for the aromatic ring.

The IR spectrum showed bands at 1400, 1450, 1520 and 1610 for compound VII indicated $\text{C}=\text{C}$ stretching vibration for the aromatic ring.

The IR spectrum showed bands at 1380, 1420, 1520 and 1600 for compound VIII indicated $\text{C}=\text{C}$ stretching vibration for the aromatic ring.

The IR spectrum showed bands at 1200, 1235, 1225 and 1210 cm^{-1} for compounds (V, VI, VII and VIII) respectively as indication of C-O stretching vibration.

The IR spectrum showed bands at (3220-3400b and 3520s) cm^{-1} for compounds (VII and VIII) respectively as indication of O-H stretching vibration.

The IR spectrum showed bands at (2920, 2990, 2900 and 2980) cm^{-1} for compounds (VII and VIII) respectively as indication of C-H stretching vibration of the aliphatic part.

3.4.4. UV spectrum of 1,4dihydro-2,6dimethyl-4-alkyl pyridine-3,5-dicarboxylic acid diethyl ester

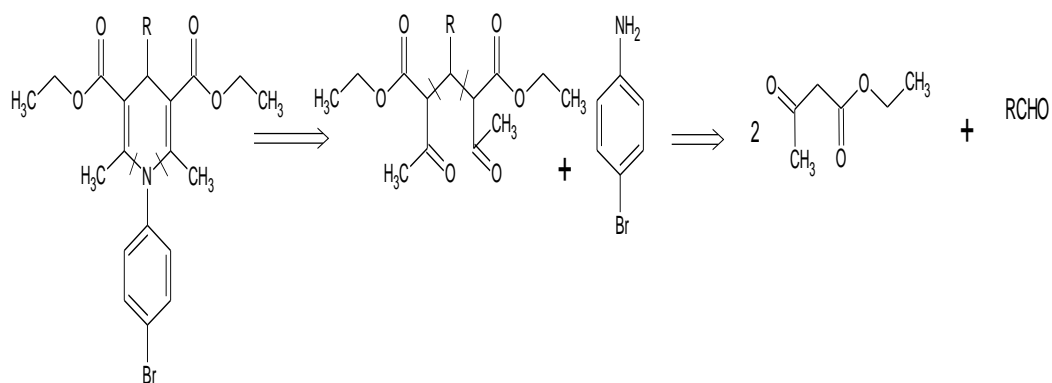
The UV spectrum showed bands at (346, 322, 298, 349) nm for compounds (I, II, III and IV) respectively as indication of $\pi \rightarrow \pi^*$ transition.

The UV spectrum showed bands at (316, 313, 340 and 326) nm for compounds (V, VI, VII and VIII) respectively as indication of $\pi \rightarrow \pi^*$ transition.

3.5. Retro-synthetic analysis of 1,4 dihydropyridine

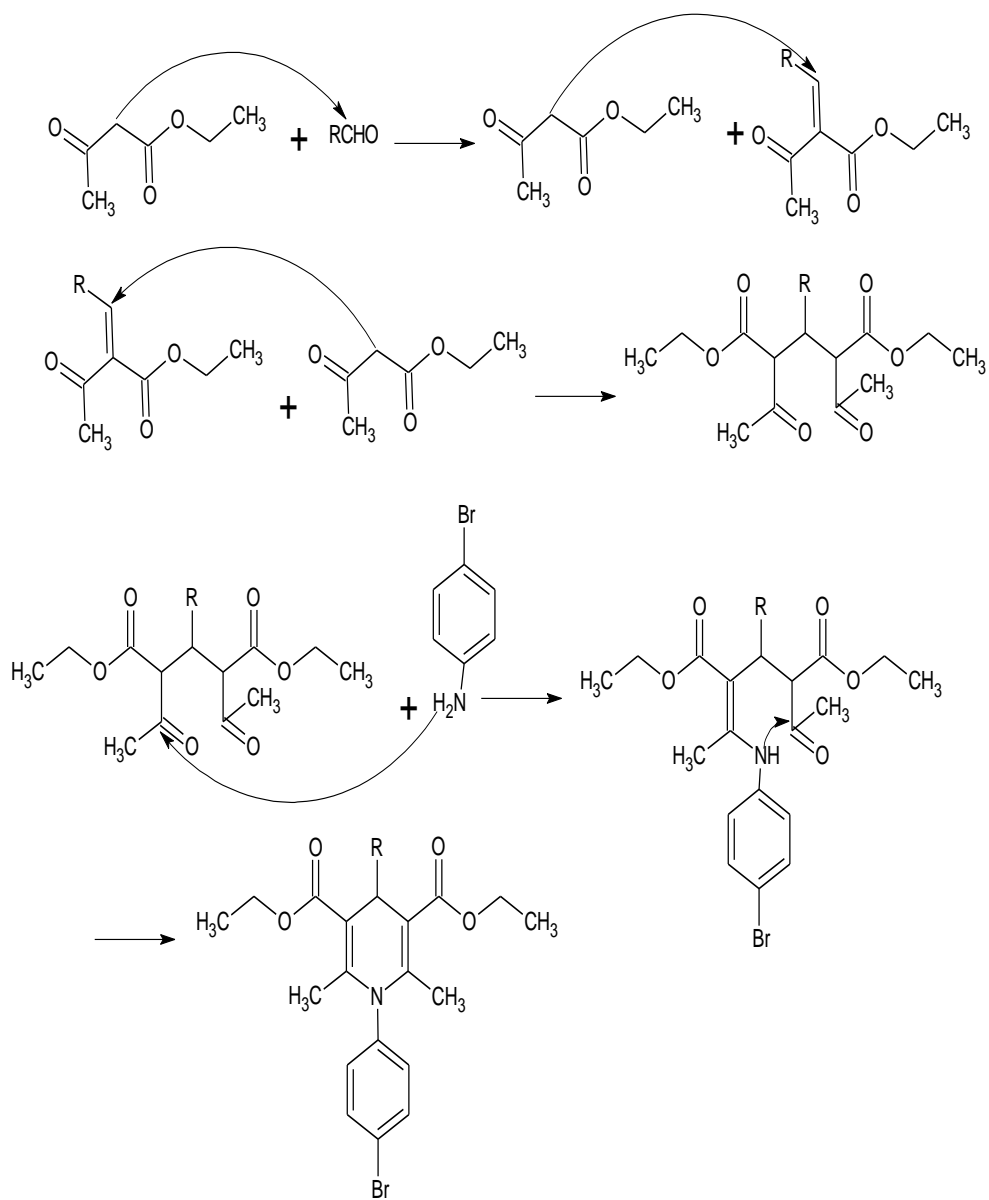
3.5.1. Retro-synthetic disconnection of N-bromo phenyl 1,4dihydro-2,6dimethyl-4-alkyl pyridine-3,5- dicarboxylic acid diethyl ester

The synthetic designing of the N-bromo phenyl 1,4dihydro-2,6dimethyl-4-alkyl pyridine-3,5- dicarboxylic acid diethyl ester in this work was adopted through the disconnection approach. The retro-synthetic analysis of these compounds can be shown below



3.5.2. Mechanism formation of N-bromo-1,4dihydro-2,6dimethyl-4-alkayl pyridine-3,5- dicarboxylic acid diethyl ester

The reaction of 2:1 molar ratio of the required Ethyl aceto acetate and the aldehyde can produce the Ia product which reacted with ammonium acetate to give the final product. The mechanism of such reaction can be illustrated below:



(Kumar *et al*, 2011)

3.6. Conclusion

After docking and QSAR Studies of 1,4-dihydropyridine derivatives as anti-cancer agent, specifically for the protein (receptor) 4o6w which affected HepG2 cells causing liver cancer were completed, the synthesized compounds have ability to act as anti-cancer agent. According to QSAR compound number XII and XX shows high ability to act as anti-cancer agent because it gives high TGI values 120 and 48 respectively, from docking compound number XXXVIII and XXXV shows high interaction with the receptor (4 interactions)

We notice that after the substitution in N-position of 1,4-dihydropyridine derivatives by sulfadoxine and sulfanilamide the interaction with the receptor increases as predicted because they have known activity against cancer cells.

After comparison synthesized compounds shows affinity approximately similar with standard doxorubicin specially compounds (VII and VIII) which (s) value -20.2331 and -20.1053 respectively compared with standard (s) value -21.6769.

3.7. Recommendation

- 1- The final product need advance characterization techniques such as NMR and Mass spectroscopy.
- 2- examine the final product in biological activity to compare it with predicted once from this work.
- 3- Recommendation to use simulation techniques in the field of synthesis.
- 4- Use other simulation techniques such as syball

References

- Ahamed, A., Arif, I.A., Mateen, M., Kumar, R.S. and Idhayadhulla, A., (2018). Antimicrobial, anticoagulant, and cytotoxic evaluation of multidrug resistance of new 1, 4-dihydropyridine derivatives. *Saudi journal of biological sciences*, 25(6), 1227-1235.
- Benigni, R. ed., 2003. Quantitative structure-activity relationship (QSAR) models of mutagens and carcinogens. CRC press.
- Clark, A. M., Labute, P. (2007). 2D Depiction of Protein-Ligand Complexes; *Journal of Chemical Information and Modelling*.(47), 1933–1944.
- Corbeil, C.R., Williams, C.I., Labute, P. (2012). Variability in Docking Success Rates Due to Dataset Preparation; *Journal ComputerAided Molecular Designing*. (26) 775–786.
- Datar, P. A. and Auti, P. B. (2016). Design and synthesis of novel 4-substituted 1,4-dihydropyridine derivatives as hypotensive agents. *Journal of Saudi Chemical Society*, 20(5), 510–516.
- Dennis Douroumis. (2015). *Computational Pharmaceutics Application of Molecular Modeling in Drug Delivery*. Wiley.
- Guide for Applying Techniques to Real-World Problems. New York (Vol. 9). <https://doi.org/10.1002/jat.1666>ubinskii, M. A. (2002). *Ultraviolet Spectroscopy And Uv Lasers*.
- Kumar, S., Idhayadhulla, A., Nasser, A., and Selvin, J. (2011). Synthesis and antimicrobial activity of a new series 1,4-dihydropyridine derivatives. *Journal of the Serbian Chemical Society*, 76(1), 1–11.
- Labute, P. (2008). The Generalized Born / Volume Integral (GB/VI) Implicit Solvent Model: Estimation of the Free Energy of Hydration Using London Dispersion Instead of Atomic Surface Area; *Journal of Computational Chemistry*.(29), 1963–1968.
- Labute, P. (2008). Protonate3D: Assignment of Ionization States and Hydrogen Coordinates to Macromolecular Structures; *Proteins* (75), 187–205.
- Lewars and Errol. (2004). *Computational Chemistry Introduction to the Theory and Applications of Molecular and Quantum Mechanics*. Kluwer Academic Publishers.
- Miranker, A., Karplus, M. (1991) Functionality Maps of Binding Sites: A Multiple Copy Simultaneous Search Method; *Proteins: Structure, Function, and Genetics* 11 , 29–34.
- molecular operating environment (MOE): application of QSAR and molecular docking to drug discovery. *Current Topics in Medicinal Chemistry*, 8(18), 1555–1572.

Phillips, J.C., Braun, R., Wang, W., Gumbart, J., Tajkhorshid, E., Villa, E., Chipot, C., Skeel, R.D., Kale, L. and Schulten, K., (2005). Scalable molecular dynamics with NAMD. *Journal of computational chemistry*, 26(16).1781-1802.

Rucins, M.,(2017). Design of pharmacophoric group containing 1, 4-dihydropyridine derivatives and determination of spectrum of pharmacological activities.

Sabljić, A. (2001). QSAR models for estimating properties of persistent organic pollutants required in evaluation of their environmental fate and risk. *Chemosphere*, 43(3), 363–375.

Saneja, A., Chetan Sharma, K.R., Aneja, R. P. (2010). Scholars Research Library. *Pharmacia*, 2(2), 208–220.

Shea, J. J. (1998). Handbook of Instrumental Techniques for Analytical Chemistry. *IEEE Electrical Insulation Magazine*, 14(6), 42–42.

Soga, S., Shirai, H., Kobori, M. and Hirayama, N. (2007). Use of Amino Acid Composition to Predict Ligand-Binding Sites; *J. Chem. Inf. Model.* (47), 400–406.

Verma, J., Khedkar, V.M. and Coutinho, E.C., (2010). 3D-QSAR in drug design-a review. *Current topics in medicinal chemistry*, 10(1).95-115.

Vilar, S., Cozza, G. and Moro, S., (2008). Medicinal chemistry and the molecular operating environment (MOE): application of QSAR and molecular docking to drug discovery. *Current topics in medicinal chemistry*, 8(18), 1555-1572.

Young, D.C., (2001). *Computational Chemistry: A Practical guide for applying Techniques to Real world Problems* John Wiley and Sons Inc. New York, USA.

Appendix

Appendix1 Descriptors which used to performing Multiple Linear Regression to obtaining QSAR equation with low R^2 value

$$R^2=0.59$$

COMPOUND NO	logP TGI	Density	molar refractivity	index of refraction	LogP
1	1.463	1.188	99.18	1.540	3.27
2	1.401	1.183	92.50	1.546	3.56
3	1.480	1.132	97.30	1.525	4.21
4	1.795	1.411	107.93	1.620	1.68
5	1.761	1.425	101.26	1.634	1.39
6	1.733	1.352	106.05	1.603	0.73
7	1.679	1.386	120.57	1.665	0.47
8	1.709	1.457	115.77	1.702	0.18
9	1.752	1.442	122.45	1.683	0.47

Appendix 2

$\log IC_{50} = 2.32 - 0.550 \text{ Density} + 0.00317 \text{ molar refractivity} + 0.04 \text{ index of refraction} - 0.0243 \text{ LogP}$

$$R^2=0.44$$

COMPOUND NO	log IC50	Density	molar refractivity	index of refraction	LogP
1	1.945	1.188	99.18	1.540	3.27
2	1.911	1.183	92.50	1.546	3.56
3	2.000	1.132	97.30	1.525	4.21
4	1.857	1.411	107.93	1.620	1.68
5	1.948	1.425	101.26	1.634	1.39
6	1.964	1.352	106.05	1.603	0.73
7	2.000	1.386	120.57	1.665	0.47
8	1.915	1.457	115.77	1.702	0.18

Appendix 3

$$\log TGI = 1.15 + 0.088 \text{ LogP} - 0.0074 \text{ molar refractivity} + 3.17 \text{ Density}$$

$$R^2=0.37$$

COMPOUND NO	logP TGI	Density	molar refractivity	index of refraction	LogP
1	1.463	1.188	99.18	1.540	3.27
2	1.401	1.183	92.50	1.546	3.56
3	1.480	1.132	97.30	1.525	4.21
4	1.795	1.411	107.93	1.620	1.68
5	1.761	1.425	101.26	1.634	1.39
6	1.733	1.352	106.05	1.603	0.73
7	1.679	1.386	120.57	1.665	0.47
8	1.709	1.457	115.77	1.702	0.18
9	1.752	1.442	122.45	1.683	0.47

Appendix 4: $-\log GI50 = -1.88 + 0.037 \text{ LogP} - 0.0039 \text{ molar refractivity} + 2.63 \text{ Density}$

COMPOUND NO	$-\log GI50$	Density	molar refractivity	LogP
1	0.000	1.188	99.18	3.27
2	1.209	1.188	99.18	3.27
3	1.181	1.183	92.50	3.56
4	1.235	1.132	97.30	4.21
5	1.494	1.411	107.93	1.68
6	1.459	1.425	101.26	1.39
7	1.439	1.352	106.05	0.73
8	1.371	1.386	120.57	0.47
9	1.444	1.457	115.77	0.18

Appendix 5

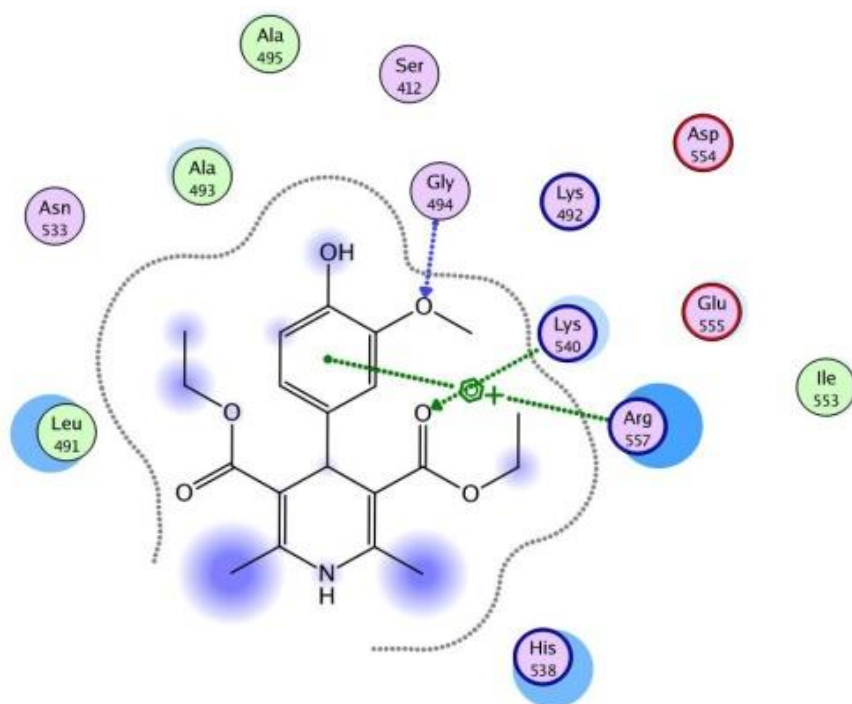
$\log GI50 = 4.09 + 0.222 \text{ Density} + 0.00228 \text{ molar refractivity} - 1.73 \text{ index of refraction} - 0.0940 \text{ LogP}$

COMPOUND NO	logGI50	Density	molar refractivity	index of refraction	LogP
1	1.684	1.188	99.18	1.540	3.27
2	1.525	1.183	92.50	1.546	3.56
3	1.488	1.132	97.30	1.525	4.21
4	1.683	1.411	107.93	1.620	1.68
5	1.714	1.425	101.26	1.634	1.39
6	1.742	1.352	106.05	1.603	0.73
7	1.808	1.386	120.57	1.665	0.47
8	1.709	1.457	115.77	1.702	0.18
9	1.679	1.442	122.45	1.683	0.47

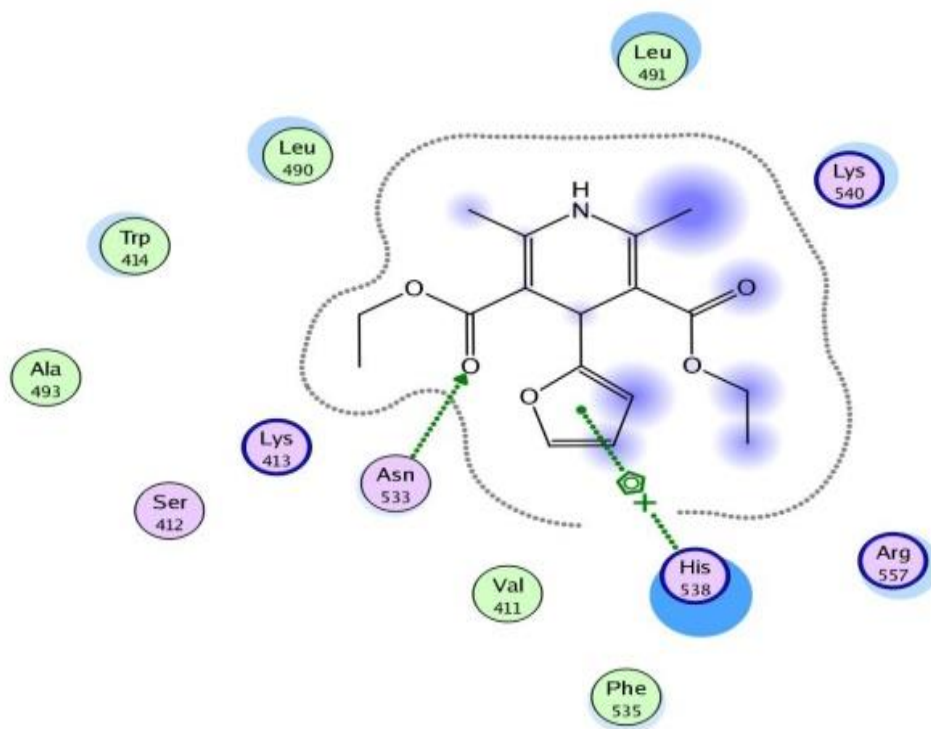
Appendix 6: $-\log GI50 = -1.88 + 2.63 \text{ Density} - 0.0039 \text{ molar refractivity} + 0.037 \text{ LogP}$

COMPOUND NO	$-\log GI50$	Density	molar refractivity	LogP
1	0.000	1.188	99.18	3.27
2	1.209	1.188	99.18	3.27
3	1.181	1.183	92.50	3.56
4	1.235	1.132	97.30	4.21
5	1.494	1.411	107.93	1.68
6	1.459	1.425	101.26	1.39
7	1.439	1.352	106.05	0.73
8	1.371	1.386	120.57	0.47
9	1.444	1.457	115.77	0.18

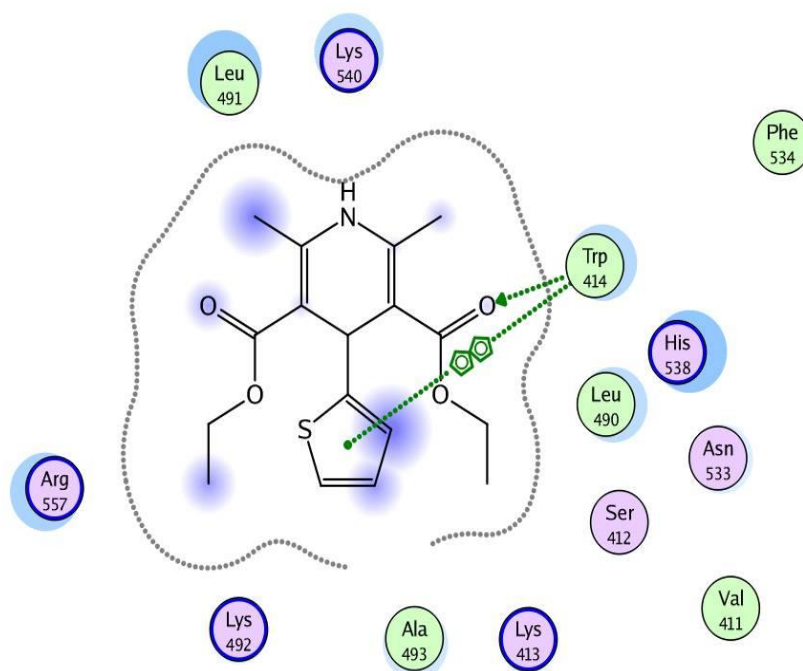
Appendix 7: Interaction between compound 5 and receptor 4o6w



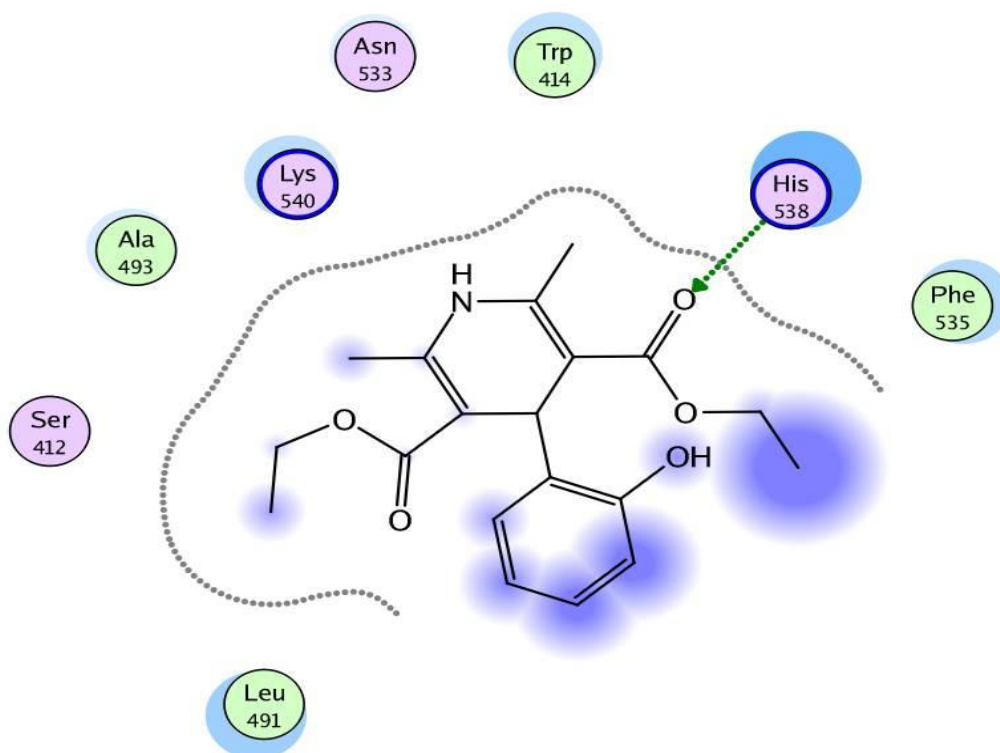
Appendix 8: Interaction between compound 7 and receptor 4o6w



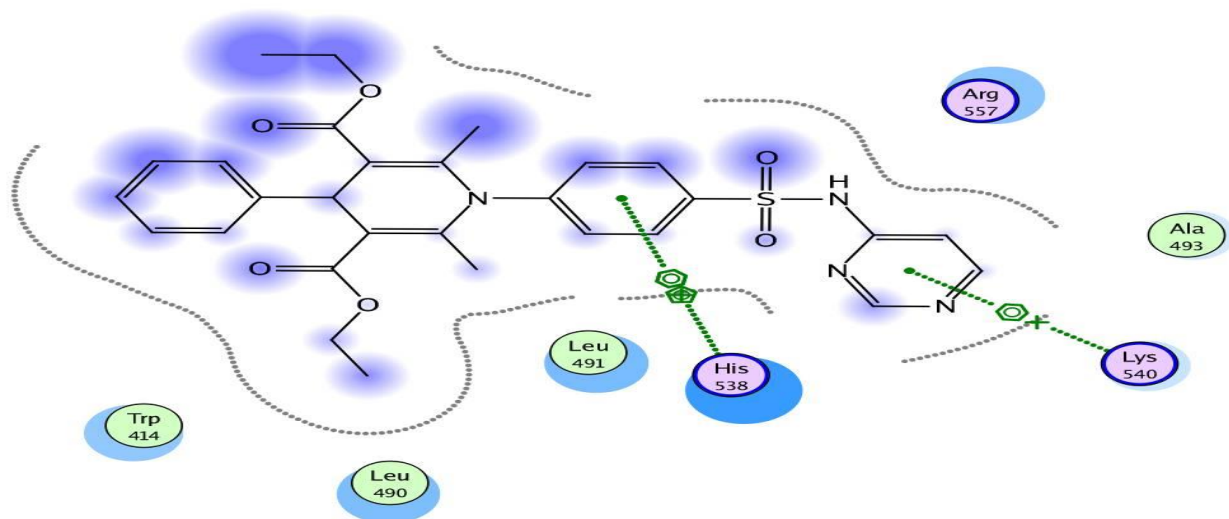
Appendix 9: Interaction between compound 8 and receptor 4o6w



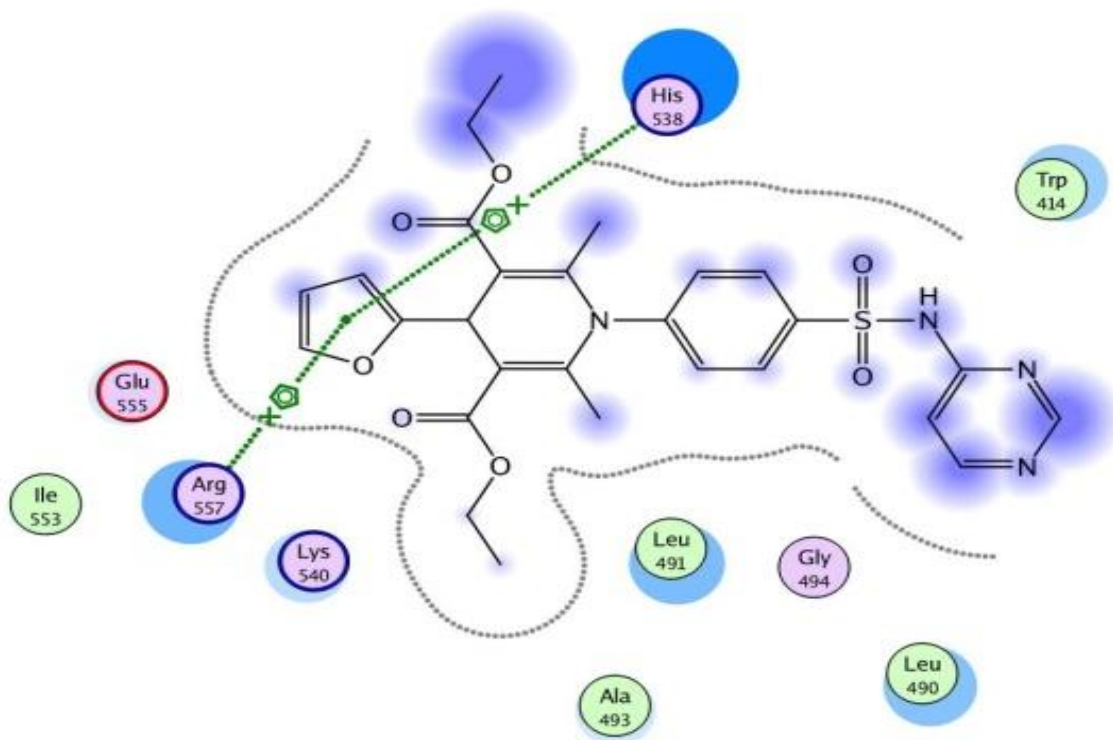
Appendix 10: Interaction between compound 4 and receptor 4o6w



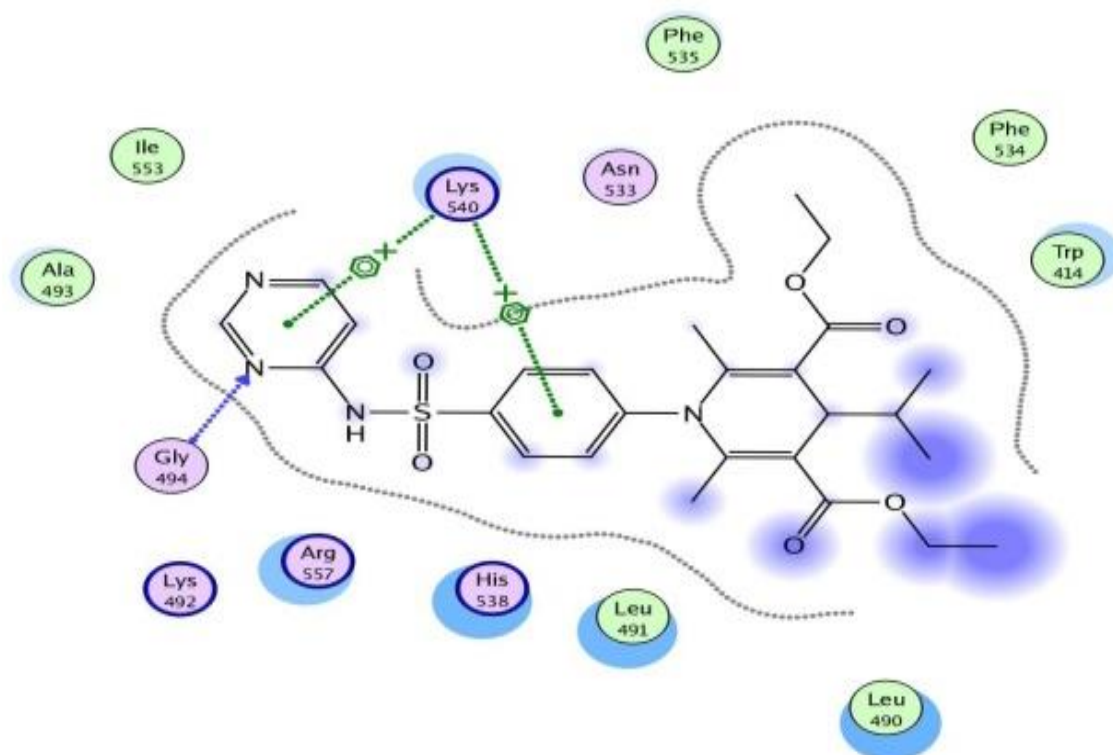
Appendix 11: Interaction between compound 23 and receptor 4o6w



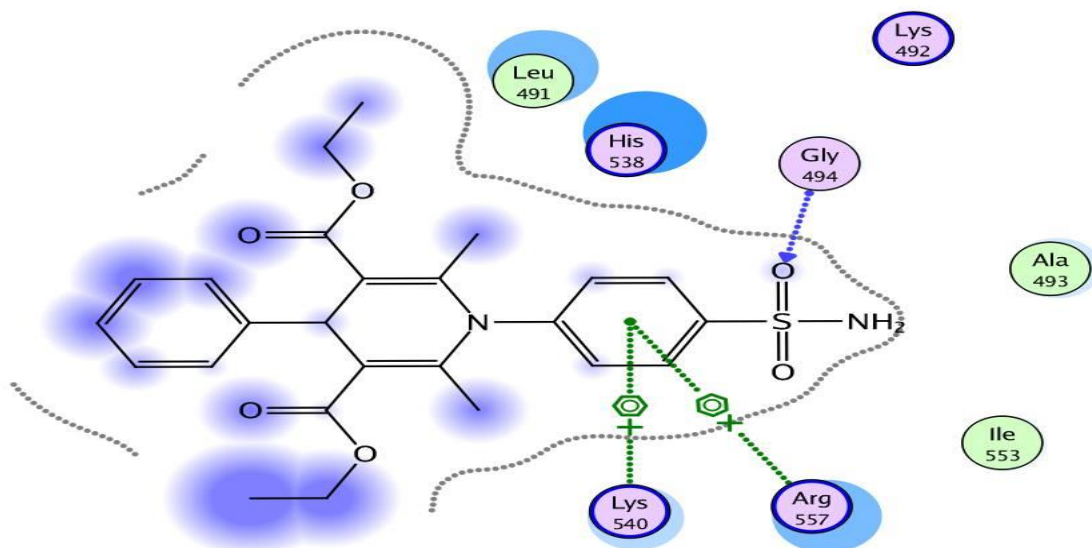
Appendix 12: Interaction between compound 27 and receptor 4o6w



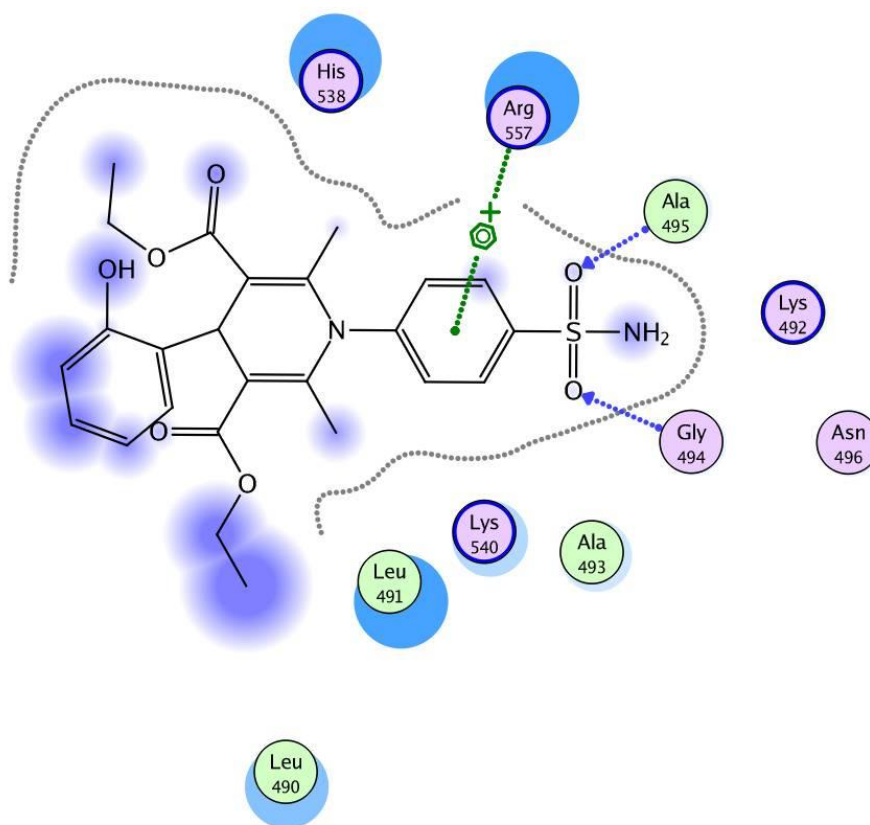
Appendix 13: Interaction between compound 29 and receptor 4o6w



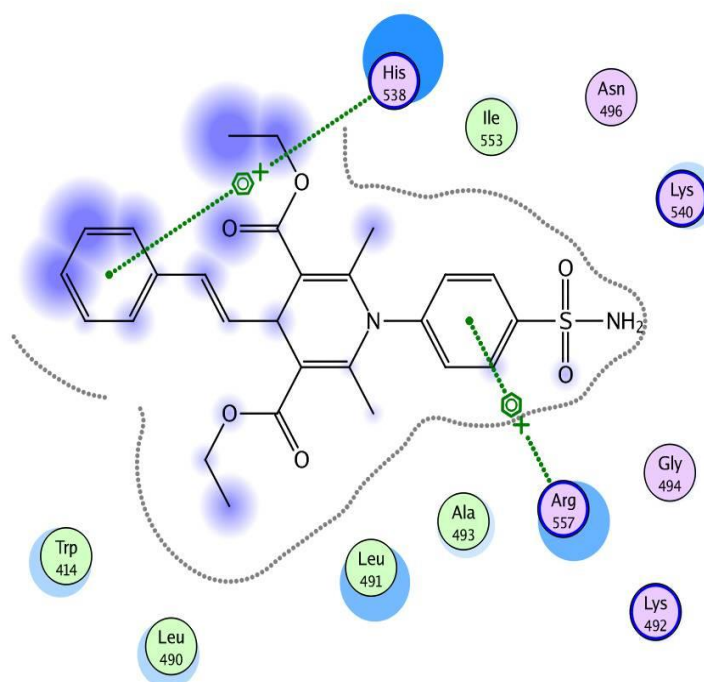
Appendix 14: Interaction between compound 33 and receptor 4o6w



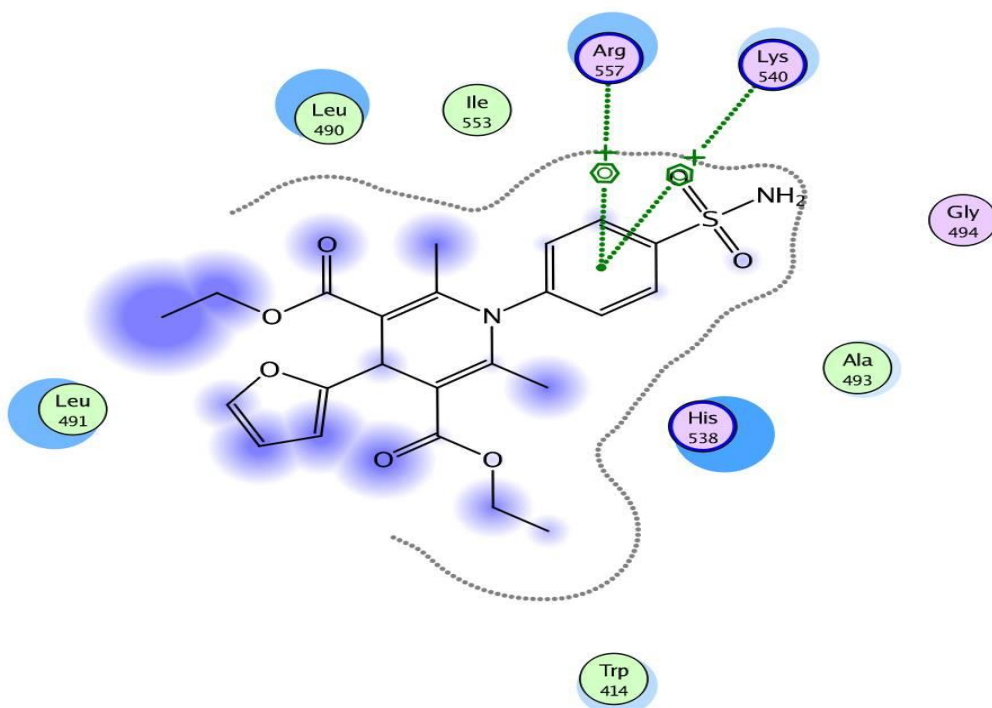
Appendix 15: Interaction between compound 34 and receptor 4o6w



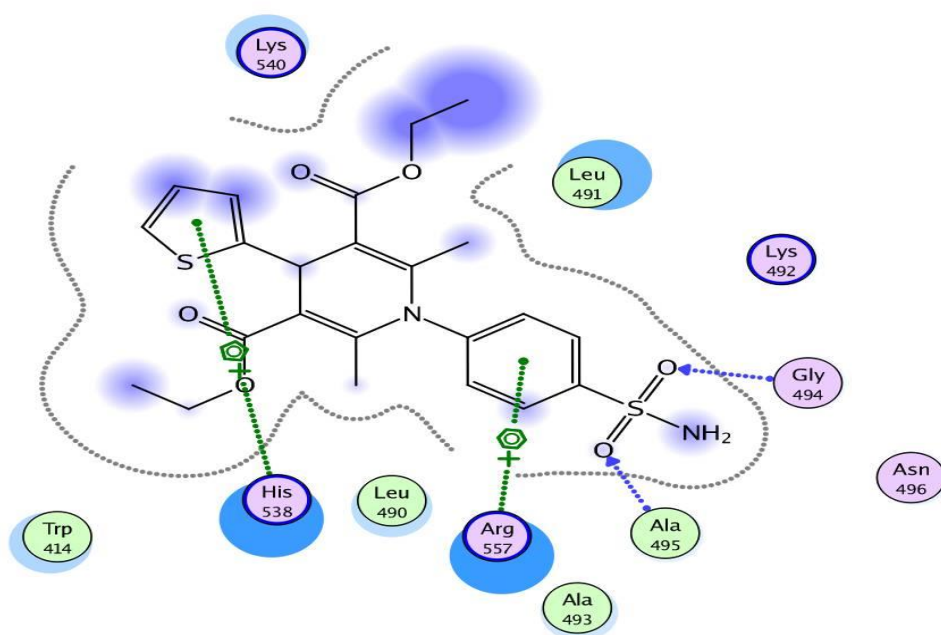
Appendix 16: Interaction between compound 36 and receptor 4o6w



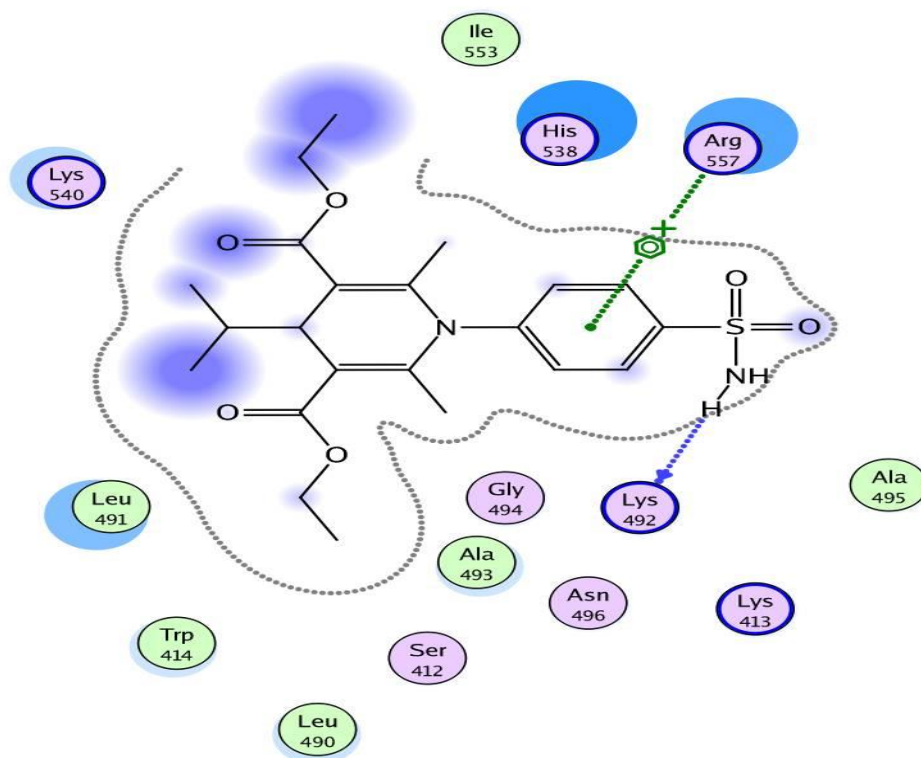
Appendix 17: Interaction between compound 37 and receptor 4o6w



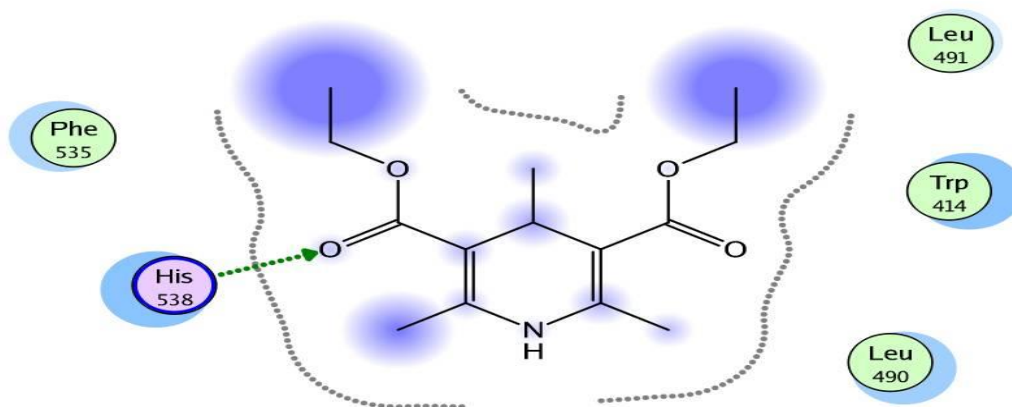
Appendix 18: Interaction between compound 38 and receptor 4o6w



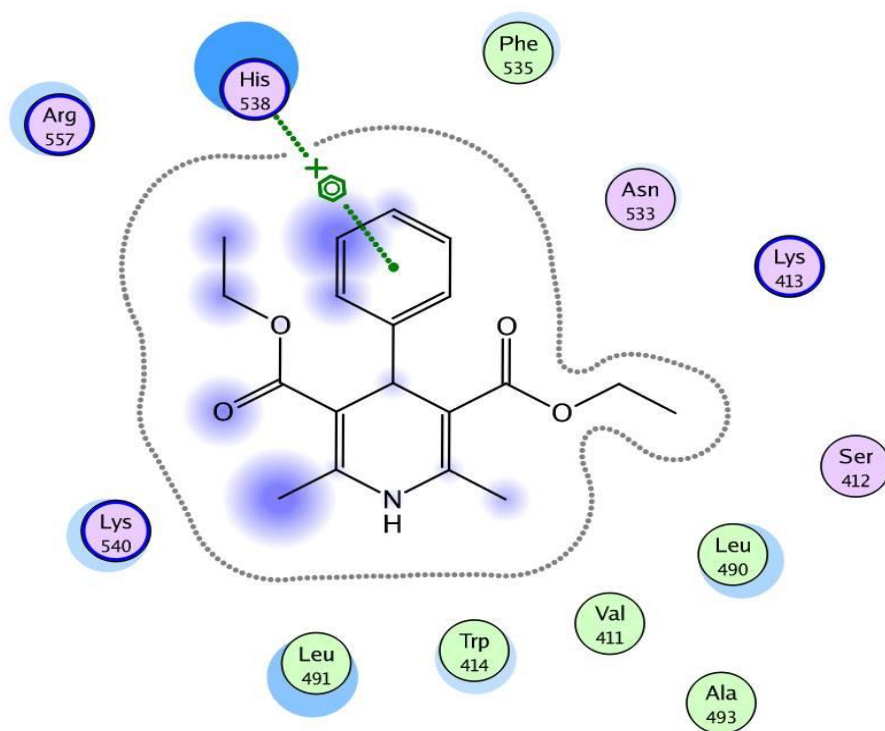
Appendix 19: Interaction between compound 39 and receptor 4o6w



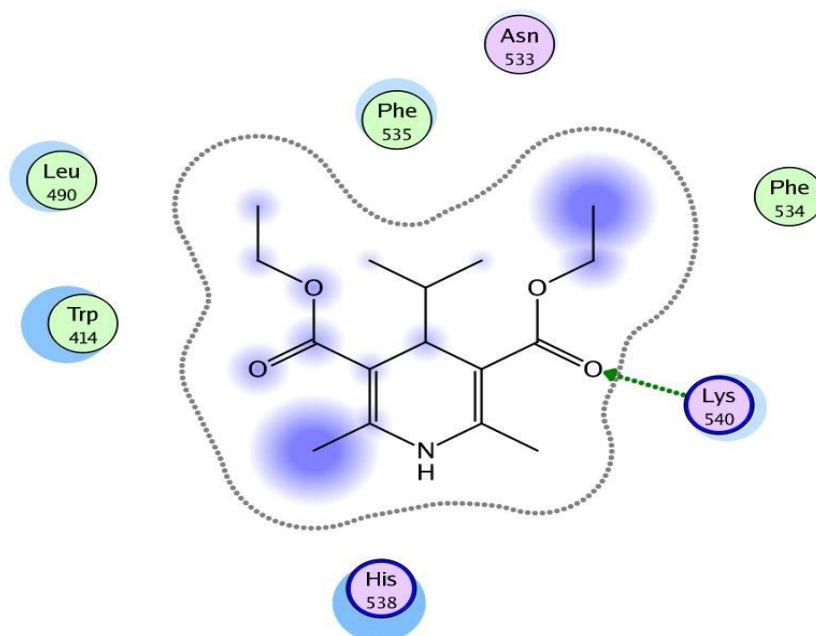
Appendix 20: Interaction between compound 2 and receptor 4o6w



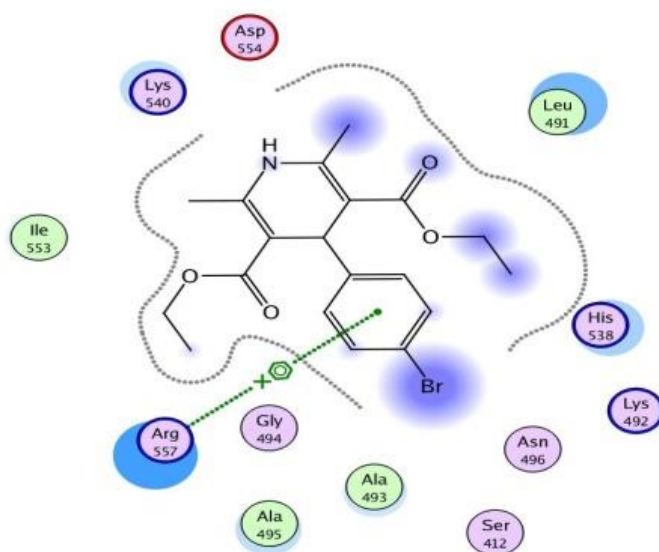
Appendix 21: Interaction between compound 3 and receptor 4o6w



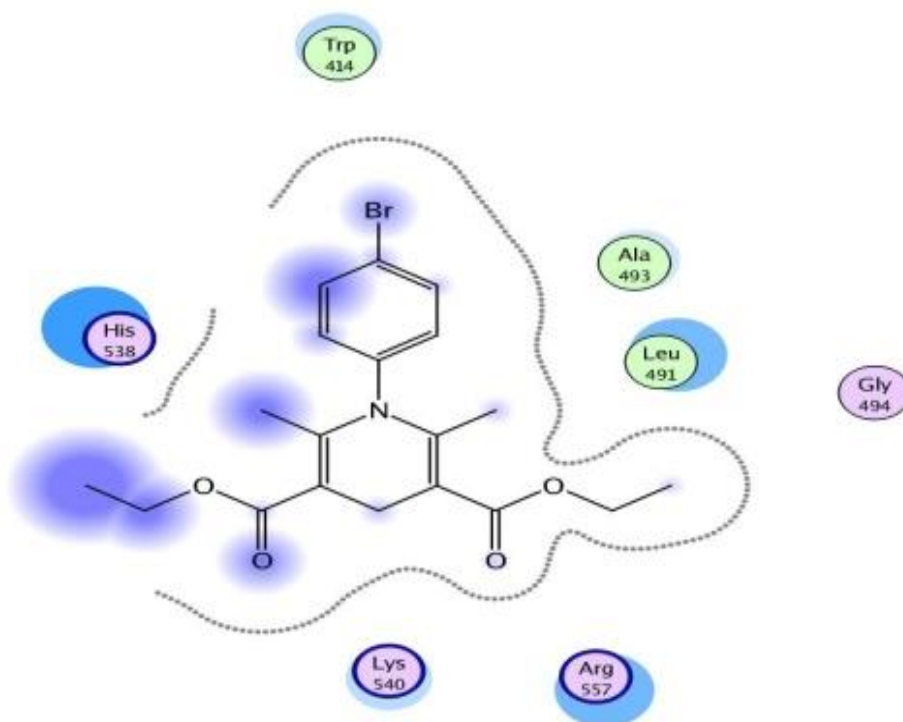
Appendix 22: Interaction between compound 9 and receptor 4o6w



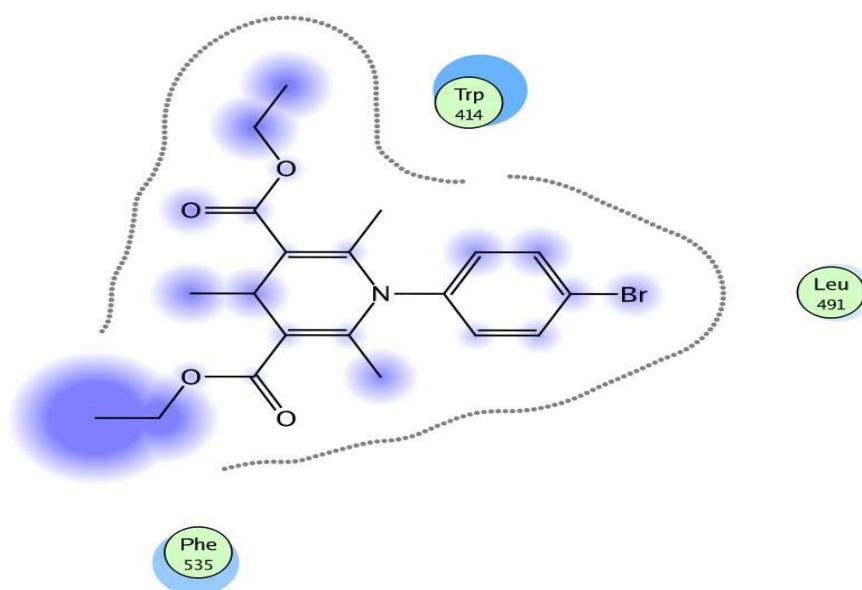
Appendix 23: Interaction between compound 10 and receptor 4o6w



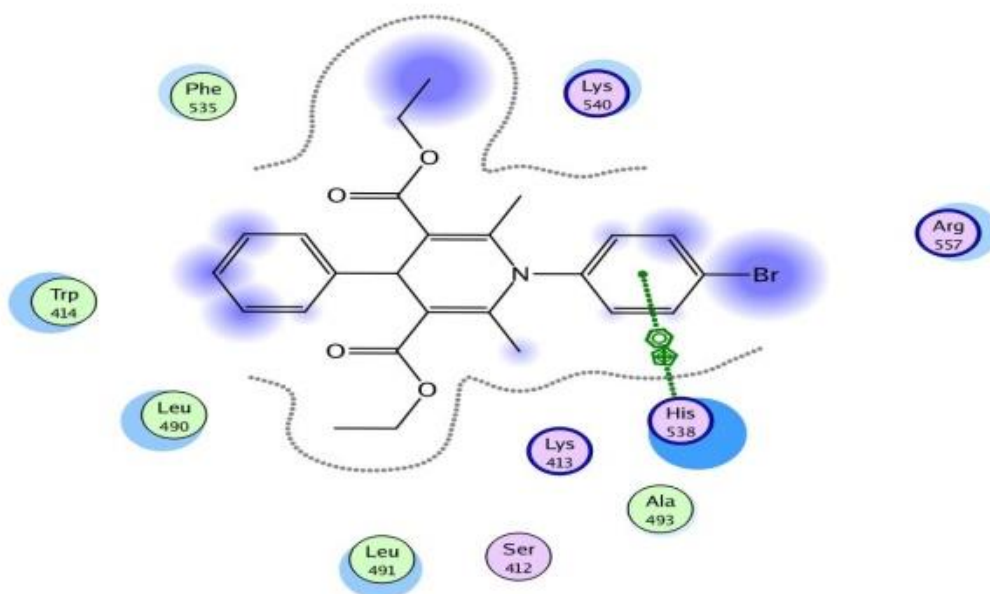
Appendix 24: Interaction between compound 11 and receptor 4o6w



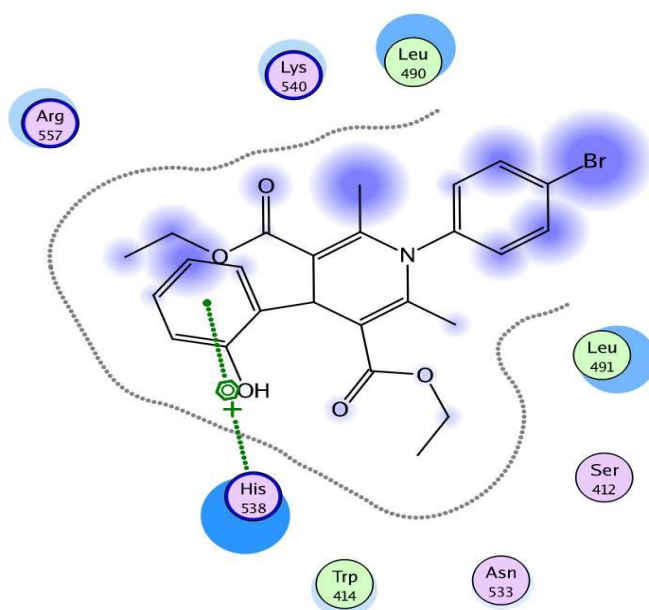
Appendix 25: Interaction between compound 12 and receptor 4o6w



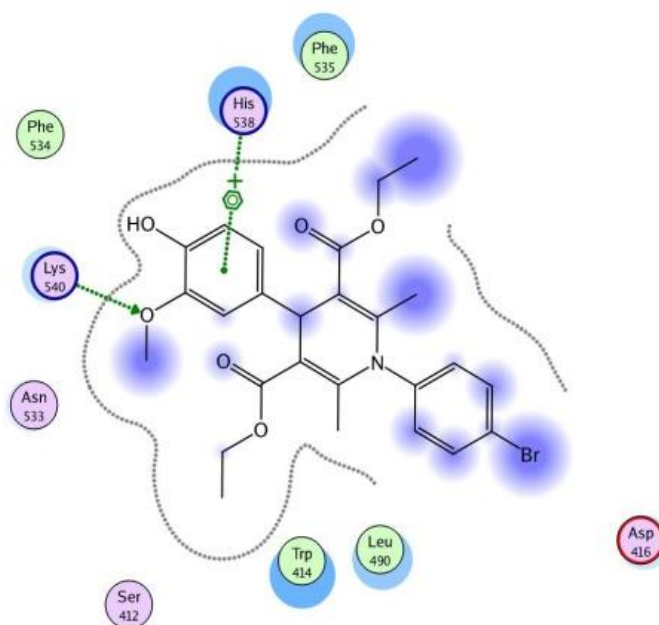
Appendix 26: Interaction between compound 13 and receptor 4o6w



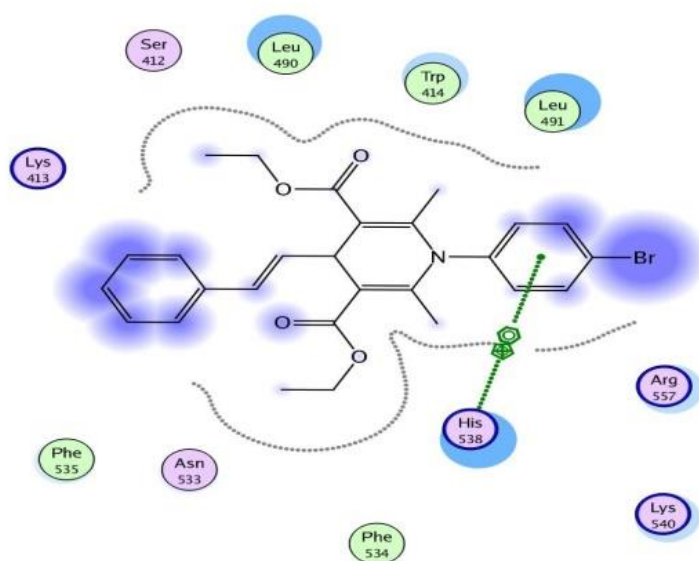
Appendix 27: Interaction between compound 14 and receptor 4o6w



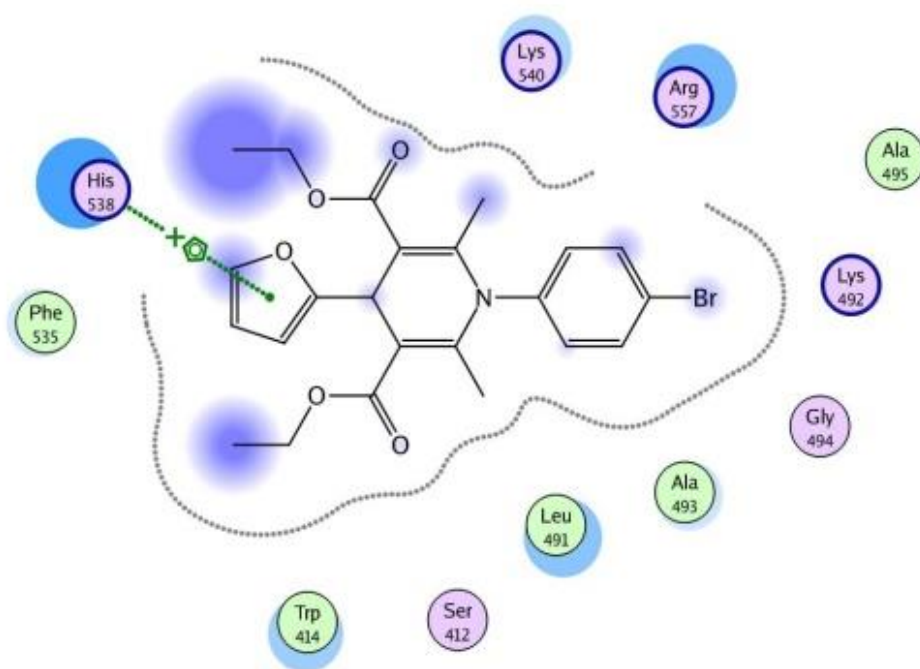
Appendix 28: Interaction between compound 15 and receptor 4o6w



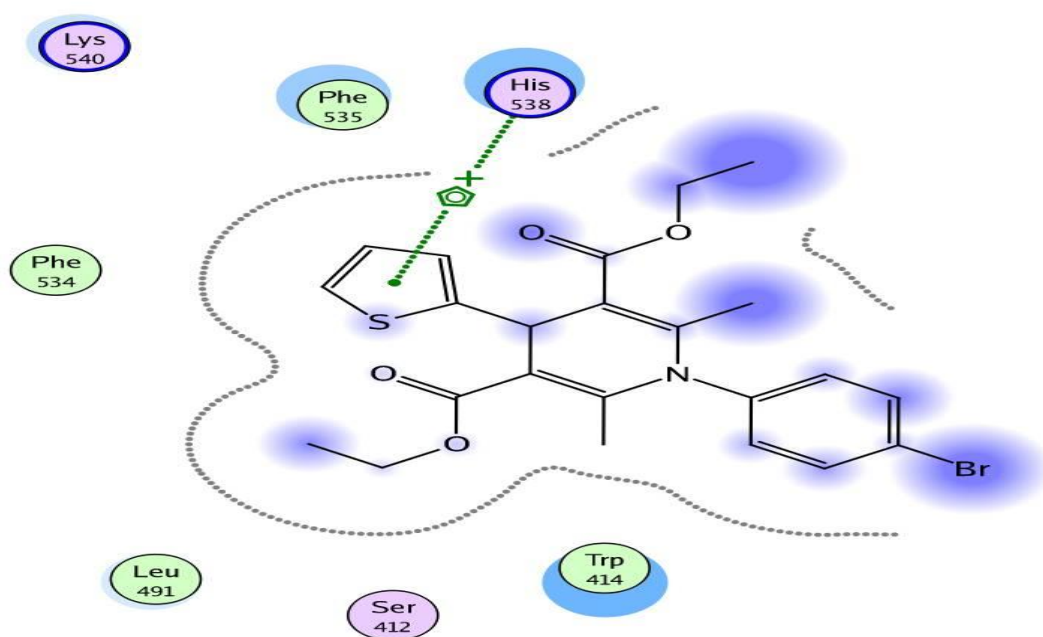
Appendix 29: Interaction between compound 16 and receptor 4o6w



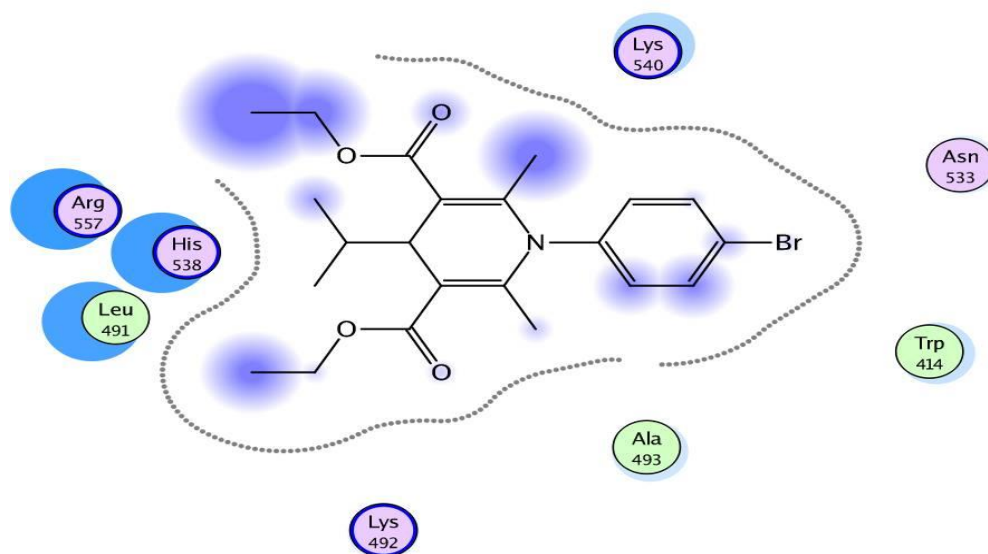
Appendix 30: Interaction between compound 17 and receptor 4o6w



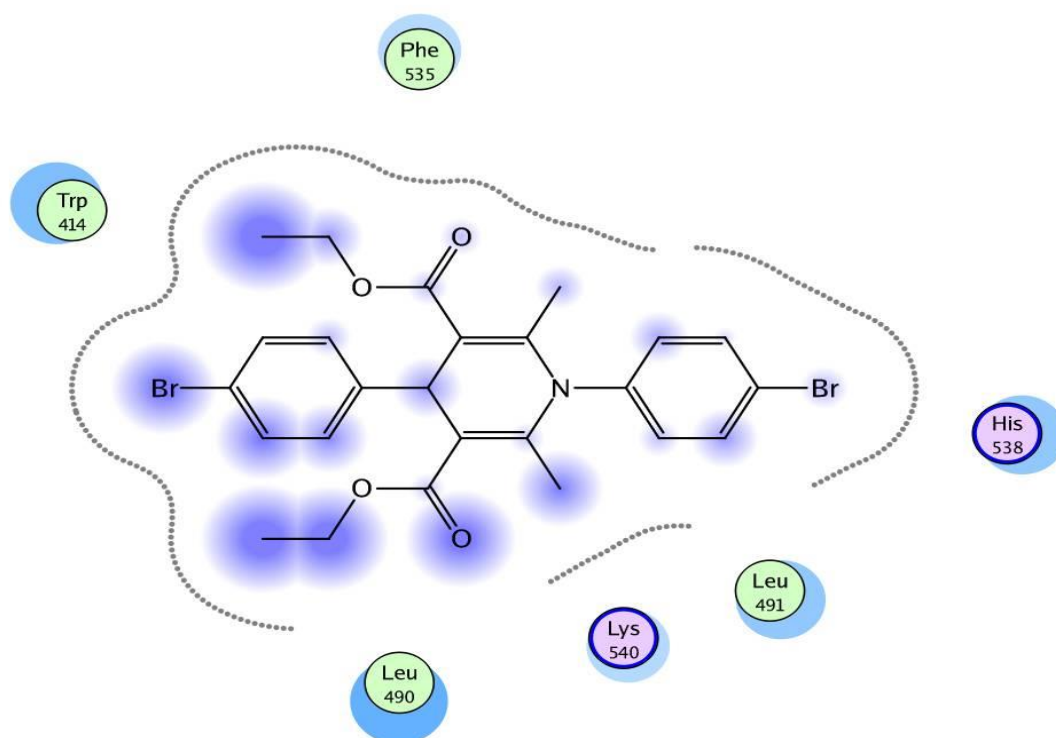
Appendix 31: Interaction between compound 18 and receptor 4o6w



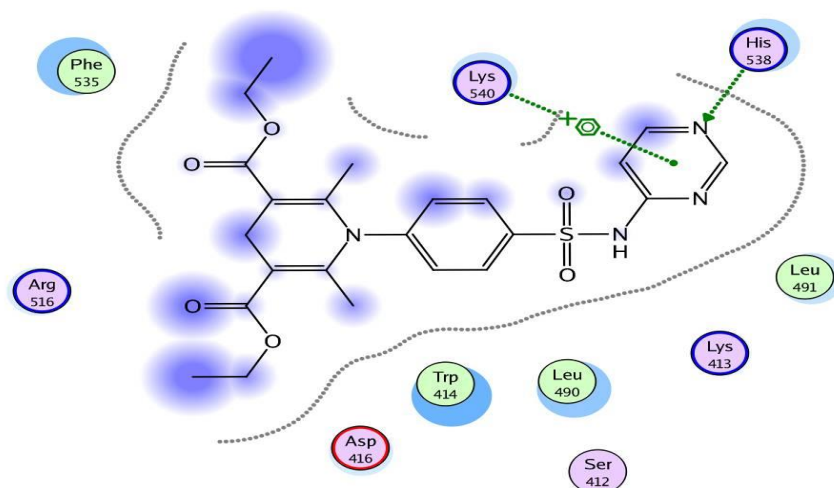
Appendix 32: Interaction between compound 19 and receptor 4o6w



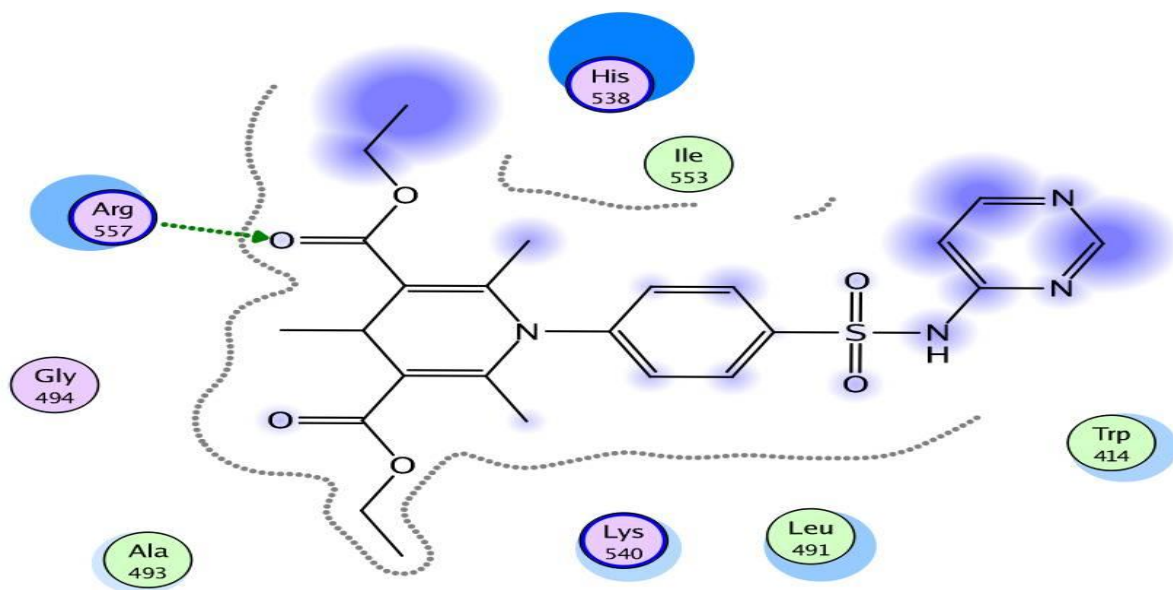
Appendix 33: Interaction between compound 20 and receptor 4o6w



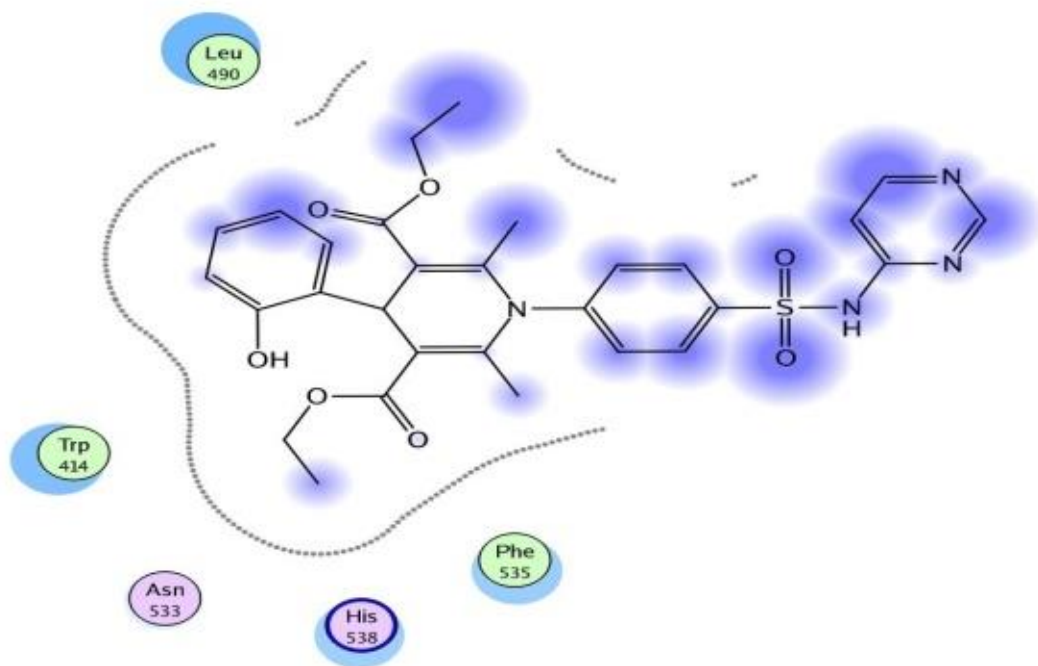
Appendix 34: Interaction between compound 21 and receptor 4o6w



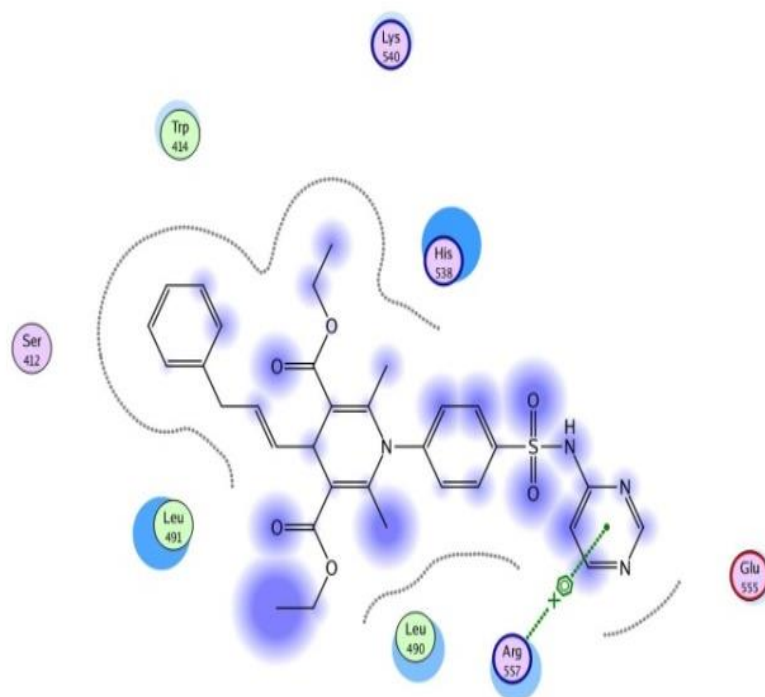
Appendix 35: Interaction between compound 22 and receptor 4o6w



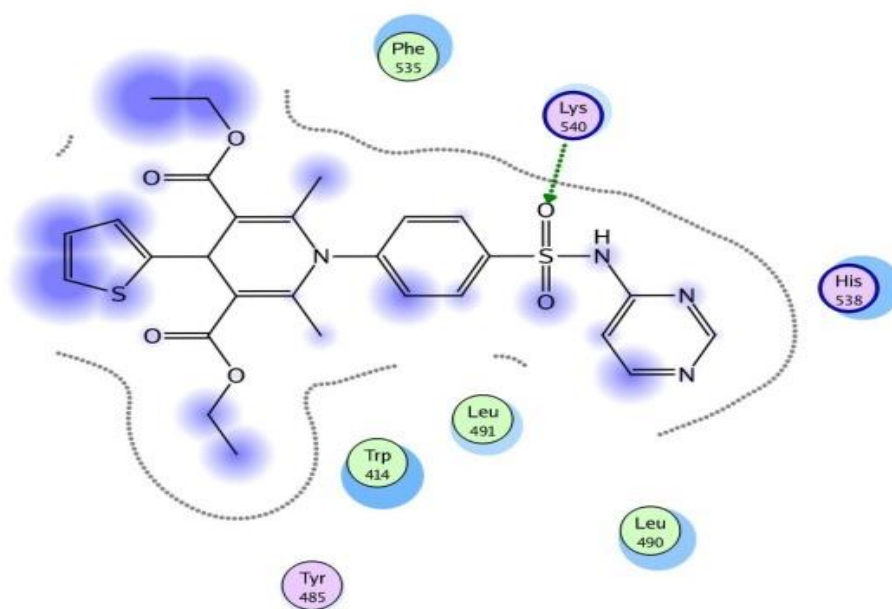
Appendix 36: Interaction between compound 24 and receptor 4o6w



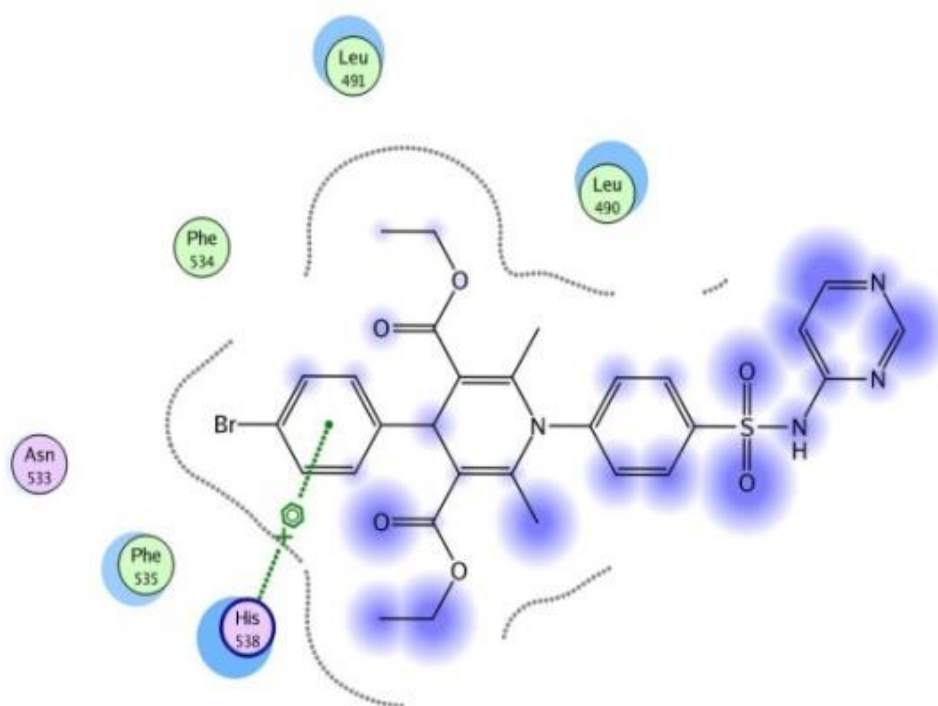
Appendix 36: Interaction between compound 26 and receptor 4o6w



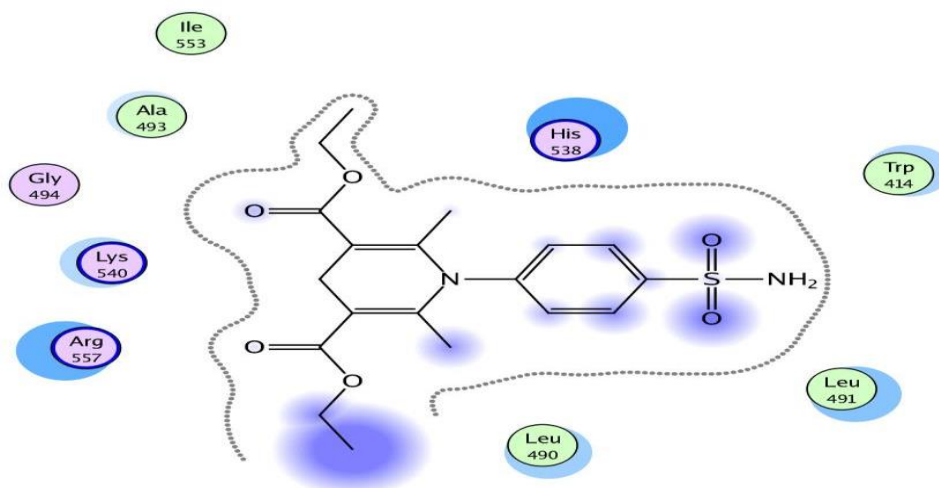
Appendix 37: Interaction between compound 28 and receptor 4o6w



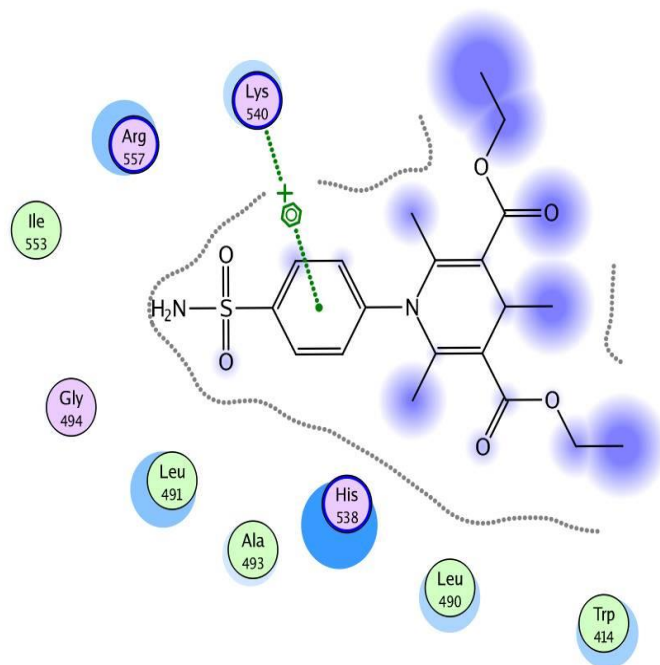
Appendix 38: Interaction between compound 30 and receptor 4o6w



Appendix 39: Interaction between compound 31 and receptor 4o6w



Appendix 40: Interaction between compound 32 and receptor 4o6w



Appendix 41: Interaction between compound 40 and receptor 4o6w

